NATURAL ENVIRONMENT RESEARCH COUNCIL

INSTITUTE OF COASTAL OCEANOGRAPHY AND TIDES

Internal Report No. 20

"Numerical investigations in the Irish Sea and its estuaries"

by M. Laska

Birkenhead-June-1970

Numerical investigations in the Irish Sea and its estuaries

A hydrodynamic-numerical model has been devised to study tides in a shallow sea.

Two-dimensional hydrodynamic-differential equations of motion and continuity, including non-linear terms, are replaced by finite-differences. The equations are in such a form that space derivatives are expressed as central differences whilst a combination of forward and backward differences is applied for time derivatives. The final equations are solved numerically on a finite-difference grid, where a step-by-step procedure in time is used.

An attempt is made to reproduce the propagation of the M_2 tide in the eastern part of the Irish Sea and to describe the behaviour of the M_2 wave in estuarial waters where a barrage crossing is proposed. The main interest is focused on tidal elevations along coasts where an increase (or decrease) of tidal amplitudes might occur in the vicinity of a barrage.

1. Introduction

In recent years the old idea of damming the entrances to shallow water areas has emerged in a new light and has been given thorough and thoughtful attention.

Proposals to construct barrages across tidal estuaries are being actively considered at national level, and at the moment a number of barrage projects are being discussed in England, by different authorities. To mention some of the schemes we may start, first of all, with the proposed barrage in the Bristol Channel, next the closure suggested for the Wash, and then the most feasible ones, namely those being considered for the River Dee, Morecambe Bay and the Solway Firth.

Reasons for building estuary barrages differ in England from site to site but, generally speaking, they are seen as means of augmenting water resources for human consumption and industrial needs, improving communications, recreational facilities, land reclamation, protection purposes and even to harness tides for power generation. Needless to say, the barrage problem is being widely investigated from various points of view. Everything is aimed at establishing objective criteria for a discussion of whether the overall potential benefits of an estuary barrage will exceed the overall costs involved. Therefore vast investigations are being carried out, involving collection and assessment of all relevant data, before the final decision to build a barrage is taken.

The whole discussion is based, as it is seen, on the following three aspects: economic and demographic, technical and engineering, and last but not

least, the hydraulic-oceanographic problem. The first two problems, although decisive in the final consideration as to whether a barrage should be erected, are beyond the scope of this report. As these two aspects play the decisive part in the final stages of ratifying a barrage project, the third hydraulic-oceanographic aspect is the initial stage of the investigation, which has to supply essential data needed in describing the best site of a crossing and the safe, yet economical, character of the structure. Apparently this will give the possibility to establish the economic and technical aspects of the whole undertaking.

It is understood that it is not our intention to argue which aspect, according to its merits, has to be given priority, for all three groups of investigation will play its own role in giving the barrage problem an expected practical realisation.

The Institute of Coastal Oceanography and Tides, formerly the Tidal Institute, being aware of the importance of the barrage problem, joined in the investigations with the purpose of tackling the problem as far as the oceanographic aspect was concerned.

A research grant, awarded by the Natural Environment Research Council in 1968, enabled the author to undertake a numerical investigation by constructing a hydrodynamic-numerical model for the eastern part of the Irish Sea and its estuaries.

It was decided that the numerical model, developed in 1961 by Lauwerier and later extended for more practical application by Heaps (1966) and Banks (1967) should be used for these investigations.

At the commencement of the study a thorough consideration was given to decide which part of the Irish Sea area should be taken into account to give the most reliable reproduction of the tidal regime, especially in the Solway Firth, Morecambe Bay and Dee River estuaries. The choice was between one model of variable mesh size, covering the entire eastern half of the Irish Sea, including its estuaries, or a group of models each covering, with a uniform mesh, a separate estuary. Giving weight to all proposals it was agreed that the first stage of the study should take the eastern part of the Irish Sea as the typical case. The decision was taken firstly due to the lack of tidal data in the mentioned estuaries and, secondly, to test the whole method on a bigger shallow sea area before commencing more detailed investigations in the Morecambe Bay, Solway Firth and Dee River. It was hoped that the first model (parent model hereafter) would provide accurate tidal data in the seaward

regions of the estuaries: data which could be used later as initial values for the small models.

Having the elevations along the open boundaries of the small models, numerical calculations would then be carried out for each estuary separately; firstly without a barrage and afterwards with a barrage crossing (in various places) in order to establish the differences, if any, in tidal regime in the estuary without and with a barrier.

It is apparent that an impermeable barrier placed across a tidal estuary will interrupt completely the normal tidal flow and may have measurable effects on the tide seaward of the structure. Thus investigations to predict the maximum sea level and current pattern seaward of a proposed barrage have to be made.

The intention of this paper is to show, in as concise a form as possible, what has been done in this field and there is no need to emphasise that it will be left to the authorities concerned to decide whether the results obtained can prove to be useful.

2. Scope of the study

The reported study was generally designed for three aforementioned areas in the eastern part of the Irish Sea, and the aim of the work was to investigate the methodology of numerical models in determining sea levels, and eventually currents, seaward of a barrage alignment.

This work, considering and applying the hydrodynamic-numerical method, is intended to set out some procedures for the application of the model as a research tool to study tides in estuarial waters and, moreover, to indicate how the numerical models can be used in supplying preliminary oceanographic data before any thorough and relevant research is undertaken.

The scope of the work is restricted not to general tidal problems as such, but to a model sea, namely the Irish Sea, where the principal lunar semi-diurnal M_2 tide is experienced as a result of co-oscillation with tides, caused by tide generating forces in the adjoining ocean.

It is worth emphasising, at the beginning, that wind stress effect, which plays a significant role in shallow sea areas, will not be taken into account in our calculations; a single M_2 constituent only will be considered.

In this work the calculations are based on the two-dimensional hydrodynamic-differential equations. These are expressed in a finite-difference form providing the basis of an iterative procedure and giving the basic

equations to forecast tidal elevations and tidal streams in the basins under discussion.

As it was said, the whole study considers the eastern part of the Irish Sea and its estuarial waters. Through the parent model investigations the open boundary input values for the small models are sought.

The given paper can be divided into three main parts. The first introductory part gives some general remarks about the barrage problem and the areas considered. The second part describes the theoretical analysis in setting and solving the given problem. Results, related mainly to the parent model and their brief discussion, are given in the third part. Results obtained in the small model investigations will be discussed in separate reports.

It is understood that some paragraphs of this report contain a number of known facts and details which were already experienced, explained, developed and solved by various investigators and, as such, could be found in literature or other sources (references given). However, they are given here for the sake of clarity and the completeness of this paper.

3. General remarks about barrages

The simplest definition for an estuary barrage can be expressed as:"a dam, permeable or non-permeable, composed generally of local materials (sand, clay, rocks) placed across an estuary in order to keep out the water of the sea." Obviously the latter is rather vague and subject to the purposes the barrage is given to serve. Thus the last part of the 'definition' changes when the tide is harnessed for, say, electric power generation.

The idea of building barrages, in British estuarial waters,is not a new one. Such barriers have been proposed in England many times, e.g. the crossing of the River Dee. Nevertheless the greatest credit has to be given, as far as the technical experience is concerned, to Dutch engineers. In this respect it is fair to mention the completion, in 1933, of the 32 km long Zuider Zee dike, and more recently the current progress of the well-known Delta Plan.

Though giving full credit to the Dutch, it is worth remarking that they were forced into such measures by their geographical position, their densely populated country and the urgent need to protect their countrymen against a recurrence of the notorious 1953 flood tragedy.

The need for barrages in Great Britain is dedicated mainly by industrial requirements. The great demand for water in this country, for industrial and potable purposes, is so far the paramount reason and inspiration for barrage building.

3·1 The barrage problem in Great Britain

As mentioned before, the necessity for estuary barrages in Great Britain is due mainly to industrial needs. Therefore all barrier structures are intended generally to be built in areas suited for such crossings, and in particular, in regions of increasing industrial activity and rapidly rising demand for fresh water.

The enclosed sketch (figure 1) shows the probable building sites for British barrages. The subsidiary figures indicate different sites, in each estuary, for proposed barrage crossings.

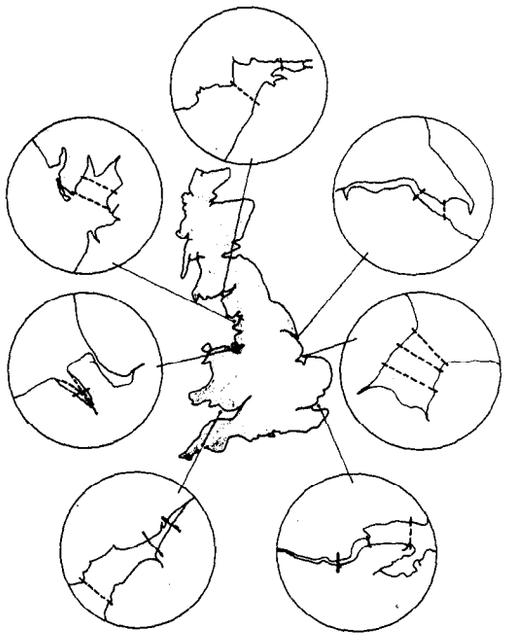

Figure 1. Suggested building sites for barrage crossings.

The best building site will be chosen, of course, after considering all the arguments for and against each possibility, once all the data required has been obtained.

It seems that some of the estuaries might have two, or even more crossings; primary and secondary ones, to achieve the most efficient exploitation of natural resources and in particular the optimal, practical solution for a proposed barrier.

No doubt all the British barrage crossings, if erected, could have many advantages, as mentioned already, but one has to bear in mind that some of the merits might be achieved at the expense of spoiling existing conditions, causing disbenefits as well: this is even without mentioning that some interests are in obvious conflict, e.g. fresh water storage and tidal power generation.

Silting or scouring problems difficulties in approaching existing harbours or even the necessity of closing some of them, flooding of agricultural land and effects on fisheries; these are only some of the considerable disadvantages which might be faced by damming an estuary. It is true to say that a barrage might cause as many problems as it solves. Therefore the whole barrage problem, as mentioned at the outset of this report, is carefully weighted and undoubtedly the fervent and dedicated enthusiasts, who can be found supporting each barrage scheme, will

always be able to establish the main reason in putting forward their barrage proposal.

The main advantage and reason for the barrages is seen to lie principally in:

(a) fresh water storage and improved communications for Morecambe Bay and Solway Firth barrages,

(b) improved communications for River Dee crossing,

(c) land reclamation and fresh water storage in the Wash project, and

(d) tidal power generation and land reclamation for barrage in Bristol Channel.

Adding to the above the flood prevention purpose for the Thames estuary barrier, one has the stimulus and all the reasons for the current barrage proposals in Britain.

4. Barrage problem in view of different model investigations

Any engineering scheme, before its final construction, has to be designed on the basis of reliable data obtained through different model investigations. Hence it appears that before a dam is erected, both the hydraulic engineer and the oceanographer will be urged to supply enough practical assessments to indicate whether the chosen estuary is suited for a barrage.

Despite a dearth of tidal data a method has to be found, and investigations carried out, to predict the water movements in a newly faced barrage situation.

As far as the hydraulic and oceanographic aspects are concerned any method applied here must provide as basic results where and how the barrage has to be placed, and how high the feasible dam has to be raised to avoid any danger of overtopping in the most adverse combination of tide, surge and waves. Interests have to be focused mainly on the changes in tidal amplitudes which might necessitate the reconsidering of existing, if any, coastal defence schemes. Only a set of relevant and comparative data collected from, say, different model investigations can give an authoritative reply on the given problem. It follows that one method of investigation does not exclude, by any means, the other but supplements it. This way of tackling a problem by various methods will be used for many years to come unless a fully proven, universal and faultless method is developed to give accurate data on the problems concerned.

For a long time there have existed some ways of tackling problems in water level variations of shallow sea areas. Tidal or non-tidal water movements have been tackled either in the hydraulic laboratory by small scale physical models, or by formulating, then solving, mathematical equations

governing the motion of the water. In the latter case it has been customary to use analytical solutions or, for simplified practical problems, an empirical or statistical method. However, the question was always open whether the results obtained by model testing techniques or appropriate mathematical methods could be accepted as accurate.

The hydraulic model investigations give, in general, a good insight into the dynamics of the water and the resultant morphology of the basin. Nevertheless hydraulic models, due to scale restrictions, cannot describe the real physical nature of the sea under consideration. Even less reliable results can be achieved, as far as the practical point of view is taken, from the analytical method. Here again all the ideal mathematical assumptions, needed to solve the given equations, restrict the derived results only to scientific understanding of the problem of interest but are doubtful for practical purposes.

In spite of all limitations confined to the results obtained by hydraulic model investigation, this has so far been the only method providing enough data for design purposes, and the results yielded by hydraulic models have generally been accepted without question. We have to admit that the latter attitude has been adopted, in some cases, because of the great cost and time involved in such investigations.

Generally speaking, it is true that water movements in a narrow estuary can be explained using small scale hydraulic models. A hydraulic model may well reproduce the dynamical regime in a narrow estuary or river channel where the geostrophic effect can be neglected. In the case of a wide estuary, however, the geostrophic motion has to be included. Therefore another approach has to be found to solve the hydrodynamical equations governing the water motion in which the geostrophic acceleration is included.

Of course it is not our aim to state which model or method has to be used. It depends on many circumstances, but it seems unlikely that a thorough investigation could ignore the hydrodynamic-numerical method which has become prominent in recent years.

It seems to the author that, if the case of a hydraulic structure to be placed in a water region arises, the hydrodynamic-numerical method (or H-N in short) should be applied as the first stage of any investigation. The author feels that the preliminary results, obtained by this method, will open the way for further research and investigation if necessary.

It should be understood that the author is far from saying that all problems concerned with water movements have to be solved by the hydrodynamic-numerical method only, but wishes to state that with the vast development of modern computing facilities the method referred to seems to be the one to give the fastest, cheapest and most reliable hydrodynamic data for use later on in any practical scheme.

If the hydrodynamic-numerical method proves capable of solving the whole problem on its own, it will be better for the method itself. If not, it can still be used to verify results from other investigations or to supply preliminary data for other methods. To describe it shortly, the H-N method, although it cannot give any information, say, about sediment transport in shallow seas, it can supply enough results on tidal elevations and tidal streams responsible for the mentioned phenomena. A hydraulic model furnished with tidal data obtained from the H-N method can then solve the relevant sediment problem. It is obvious, further on, that hydrographic data obtained in the laboratory can be used in numerical investigations, and the latter can supply the former with other results, e.g. open boundary conditions.

These small examples show only some of the many possibilities which can be matched and linked within two different models in providing relevant data. Thus hydraulic and oceanographic problems raised by a barrage structure can be easily and satisfactorily solved. Once more the statement (Rossiter, 1961) that there is a place for different models in attacking sea water dynamics has proved its value.

4·1 Hydrodynamic-numerical method

The development and availability of high-speed electronic computers has made possible the use of hydrodynamic-numerical methods for sea dynamic computation.

The H-N model investigations are now well advanced and many oceanographic problems have been so far explained and solved using this method.

The H-N method developed in 1956 by W. Hansen, the recognised pioneer in this field, has subsequently been successfully used by many investigators in studying sea level changes of tidal and non-tidal origin.

The encouraging results so far obtained by means of H-N models in reproducing tides and storm surges, by explaining their generation and propagation, has revealed the great potentialities of this method to many oceanographic problems.

The method under discussion is based on the fundamental laws of motion and continuity. Therefore the initial stage in the H-N method is the formulation of the relevant hydrodynamic-differential equations which govern the motion of the sea. The equations can be written in linear or non-linear form and are usually vertically integrated from the bottom to the surface. Such equations give us the fundamental prediction equations. To solve the given hydrodynamic-differential equations, which can be formulated in a one, two or three-dimensional system, a numerical solution is applied.

A numerical solution of the hydrodynamic-differential equations can be achieved by approximating the differential quotients by finite-differences at discrete points in time and space. This means that each partial differential coefficient has to be replaced by a finite-difference. What kind of finite-differences will be used depends on the computational scheme chosen.

In the finite-difference representation of the differential equations, central differences are most widely used to express space derivatives, while time derivatives are frequently expressed in forward or backward difference form. Such time differences will transform a situation at time t into a situation at some later time $t+\Delta t$ (where Δt is the elementary time step); the transformation only requiring information from these two time levels. Thus tides or storm surges can be built up numerically, at a series of time levels, starting with an initial state of displacement and motion.

A numerical sea model, describing in numerical terms the physical properties of a natural basin, is the only model so far which can reproduce, with sufficient accuracy, the dynamics of the water in the considered sea area. How thoroughly the sea dynamics will be reproduced depends on the accuracy in formulating the basic hydrodynamic-differential equations, on the chosen dimensions of the finite difference grid, and on the confidence which can be placed on the hydrographic and meteorological data obtained.

Whether all the mentioned 'parameters' can be included and taken in their most reliable and accurate form depends again on the data and computer core memory available.

More detailed information about the H-N models can be found in the next paragraphs, where the whole theoretical analysis, of the method under discussion is given.

5. Physical characteristics of the areas considered

It lies far beyond the scope of this report to give a complete physical account of the sea regions considered. Nevertheless, a short description of the geometrical and hydrographical properties of the basins mentioned may elucidate the problems involved.

Drawing one line from Barrow Head (Scotland) to Ayre Point (Isle of Man) and another from St. Mary (on the same island) to Carmel Head (Anglesey) we produced the western boundary of the eastern part of the Irish Sea. Taking the boundary in such a way we obtain two entrances; the northern approximately 29 km and the southern approximately 72 km wide. Through these two openings comes the tidal wave. And it is here where the amplitudes and phases of the M_2 constituent are prescribed for our computations.

The total sea area covered by our computational mesh, for the parent model, amounts to 14412 km^2. The depth distribution, in this area, varies from a maximum depth of 69·20 m. to a minimum of 5.00 m. The average depth does not exceed 25 m, giving in total a rather shallow reservoir.

Though the western boundary of our sea is a straight one, the eastern boundary is rather complicated. Here the sea enters the land in many places giving a changing coastal configuration. The sea and the entering rivers build up, in this part of the Irish Sea, many bay-like water areas. The main ones are, of course, the Solway Firth, Morecambe Bay and the Dee Estuary.

The Solway Firth with its converging coastal lines seems the easiest basin to deal with in describing the bathymetry but, oddly enough, this region is the least documented area as far as hydrographic data is concerned. More information can be found for the other two water areas, where recently some field measurements and aerial surveys were carried out. Even so, a thorough reproduction of the coastline in either of these estuaries by a "zig-zag" approximation is difficult to obtain since the coastline changes in time with water level. In Morecambe Bay, for example, at low tide about 70% of the upper reaches of the Bay are dry having only the water, confined to small channels, given by the river discharges. Most certainly these drying banks, exposed during the receding tide, are the main concern in establishing the depth values. The same concern applies to the Dee Estuary and the Solway Firth.

The tidal movement, in any of these estuaries, is very strong and produces a lot of cutting and replacement of the bottom. Thus a remarkable and surely unpredictable sediment movement occurs in such regions.

The tidal streams, during the first stages of flooding, follow the direction of the main channels. This could be said also when the banks are dry and

the ebbing tide is at its final flow. When the tide covers the banks the stream tends to run across them. It is difficult and unwise, therefore, to accept any fixed stream pattern since the bottom floor decides the direction of the tidal current (at low water) in existence.

6. General description of tides in the Irish Sea and its estuarial waters

As mentioned already the whole work deals with one principal tidal constituent only. Thus, in the following general description of the tides in the Irish Sea, we shall be mainly concerned with the principal semi-diurnal M_2 tide.

It is a known fact that tides in the Irish Sea are caused by an influx and efflux through the Northern Channel in the north and St. George's Channel in the south.

The tide generating forces (varying forces of the gravitational attraction due to the moon and the sun) which generate the tides in the Atlantic Ocean are practically negligible in the Irish Sea. It is apparent, therefore, that tides in this basin are of a co-oscillating type with those of the Atlantic. Although that type of tide seems, in general, to be a comparatively simple one, the tides in the Irish Sea are rather complex due to shallow water interactions.

It is clear that tides in the Irish basin are determined by the distribution of tidal currents over the mentioned entrances. According to Doodson and Warburg (1941) the tidal streams entering through the North Channel are at their maximum speed at 0750 in lunar time. The same applies to the tidal streams crossing the southern entrance. It means that at that time the Irish Sea begins to augment its water volume. The latter reaches its maximum amount after 3 hours, i.e. 1050 after the transit of the moon at Greenwich. The time of maximum amount of water in the basin is also the time when the currents are turning to leave the basin.

After another 3 hours the currents, at their leaving stage, reach their maximum speed. At the time of maximum speed of the currents, either inwards or outwards, one can find the mean amount of water in the Irish Sea.

The speed of the tidal currents at both openings determines the excess of the water over the referred mean volume. The current velocities differ, of course, from springs to neaps and can be strengthened or weakened by meteorological effects and, in some places, even by river discharges.

The current pattern and velocity distribution vary from site to site but generally it is accepted that the stream lines, passing the northern and southern approaches, turn in the easterly direction building up elevations along the eastern sea edges. This gives in result a surface gradient with higher water level at the English and lower at the Irish coast. Needless to say the ebb currents follow the same way, in the opposite direction of course.

The Isle of Man, being located roughly in the centre of the Irish Sea, separates, and retards to a certain extent, the meeting of the main stream flows until they reach the eastern part of the sea. The location of the island, and the depths between it and the Irish coast, is the main reason that in this region, the tidal currents are very weak and the sea area west of the island is considered as slack water.

The speed of the tidal currents, except in the slack water region, differ from place to place. The currents attain their maximum speed, as it was said before, roughly at 8 hours after the moon's crossing of the meridian of Greenwich and are the cause of building up elevations above or below the mean level. Observations show that at the eastern coast the tidal amplitude is 3·0 m (Proudman, 1953).

In the eastern half of the Irish Sea the co-range lines are 'parallel' to each other, starting with the amplitude of 220 cm. at the western border, and ending with 300 cm. at the Lancashire coast. This indicates a distinct gradient of elevation in the eastern direction.

The value of the amplitudes rises going inwards along the existing estuaries. There the increase in tidal friction, due to shallow water, causes additional growth of the tide.

Considering now the tidal range of spring and neap tide, and not the mean tide as in the case of the mentioned amplitudes, the values reach (on the southern coast of Morecambe Bay) approximately 9·0 m. and 5·0 m. respectively. A slight increase in these values may be found on the coast of the Wirral peninsula.

Adding on the astronomical tide to the meteorological tide, due to wind and pressure, one can focus interest on the height to which a barrage must be raised to withstand the head of the water (static pressure) and the wave action (dynamic pressure) likely to occur.

Figure 2 shows a chart of co-tidal and co-range lines of the whole Irish Sea. It was prepared using the classical tidal chart devised by Doodson and Corkan (1932) and data from other sources available.

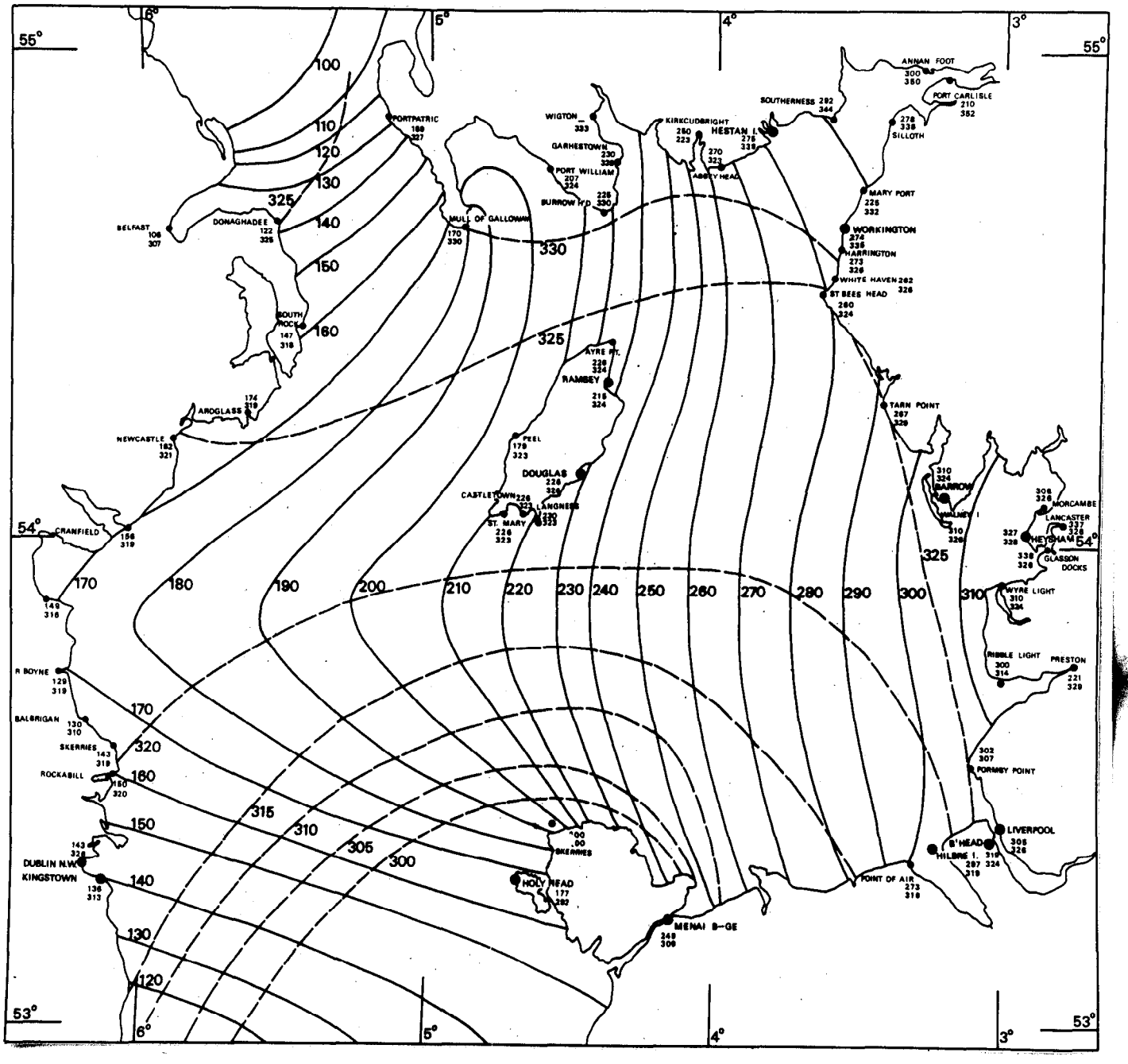

Fig. 2. The co-tidal and co-range lines of the M_2 tide in the Irish Sea (----- co-tidal (deg.), ----- co-range (amplitudes cm) lines).

The enclosed chart comprises, besides the layout of times and amplitudes of the M_2 wave, a series of H and g values for different coastal stations. The reliability of these values, collected from different sources such as: Doodson and Corkan (1932), Tidal Institute harmonic analyses, I.H.B. tables, depends on the span of data taken in evaluating H and g.

7. Theoretical analysis of the hydrodynamic-numerical investigation of the tides in shallow sea areas.

The basic mathematical analysis of difference method can be found in various publications, e.g. Buchingham (1957), Richtmeyer (1957), Collatz (1960).

The model discussed here is based on the finite-difference interpretation of the two-dimensional equations described by Lauwerier (1961), Heaps (1966) and Banks (1967). In particular the numerical scheme devised by the latter was applied, with some modifications, for the investigation under discussion.

In the hydrodynamic-differential equations applied in our model the space derivatives are expressed in central difference form. Forward differences are utilised in the equations of motion for time derivatives but, to maintain stability, the time derivatives in the equation of continuity are expressed by backward differences.

In this way the final hydrodynamic-differential equations of motion and continuity, including non-linear terms, are replaced by finite-difference equations and an iterative procedure is used for the calculation of stream components and elevation at grid points of a mesh covering the sea.

7·1 The basic hydrodynamic equations

A small sea area is considered and therefore, to facilitate the whole theoretical analysis of the given problem, the following Cartesian co-ordinate system is chosen, figure 3.

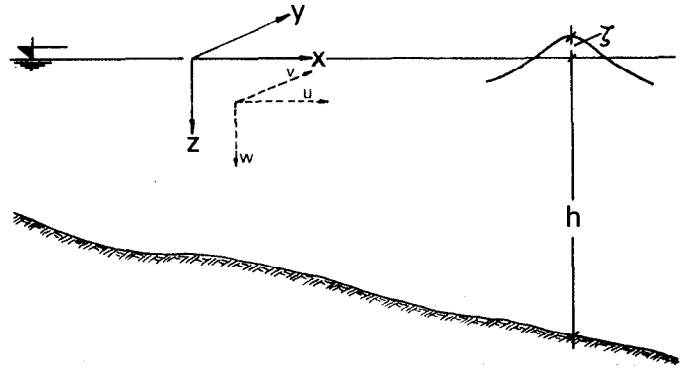

Figure 3. The chosen co-ordinate system

Assuming that the water is incompressible and homogeneous, and that the horizontal component of the geostrophic acceleration (proportional to w) is neglected; assuming, further, that of the frictional stresses acting on the water only those acting on horizontal faces are included, the general equations of motion and continuity for a rotating sea can be expressed, as follows (Defant, 1961):

$$\frac{Du}{Dt} = \frac{\partial u}{\partial t} + u\frac{\partial u}{\partial x} + v\frac{\partial u}{\partial y} + w\frac{\partial u}{\partial z} = fv - \frac{1}{\rho}\frac{\partial p}{\partial x} - \frac{1}{\rho}\frac{\partial F}{\partial z}, \qquad (1)$$

$$\frac{Dv}{Dt} = \frac{\partial v}{\partial t} + u\frac{\partial v}{\partial x} + v\frac{\partial v}{\partial y} + w\frac{\partial v}{\partial z} = -fu - \frac{1}{\rho}\frac{\partial p}{\partial y} - \frac{1}{\rho}\frac{\partial G}{\partial z}, \qquad (2)$$

$$\frac{Dw}{Dt} = \frac{\partial w}{\partial t} + u\frac{\partial w}{\partial x} + v\frac{\partial w}{\partial y} + w\frac{\partial w}{\partial z} = -\frac{1}{\rho}\frac{\partial p}{\partial z} + g, \qquad (3)$$

$$\frac{\partial u}{\partial x} + \frac{\partial v}{\partial y} + \frac{\partial w}{\partial z} = 0; \qquad (4)$$

where:

x,y,z - Cartesian co-ordinates (LHS);

u,v,w - current components in the directions of increasing x, y, z respectively;

p - pressure at a point in the water;

ρ -density of the water (assumed uniform);

g - acceleration of the Earth's gravity;

t - time;

f - Coriolis parameter ($2\omega \sin\varphi$);

F,G -components of the frictional stresses.

Considering only 'small' motion in the sea, we can neglect all terms which contain products of the velocity components u, v and w, this means that the equations can be linearised. Thus instead of D/Dt we can write $\partial/\partial t$, so that equations (1), (2) and (3) can be written in the simplified form:

$$\frac{\partial u}{\partial t} = fv - \frac{1}{\rho}\frac{\partial p}{\partial x} - \frac{1}{\rho}\frac{\partial F}{\partial z}, \qquad (5)$$

$$\frac{\partial v}{\partial t} = -fu - \frac{1}{\rho}\frac{\partial p}{\partial y} - \frac{1}{\rho}\frac{\partial G}{\partial z}, \qquad (6)$$

$$\frac{\partial w}{\partial t} = -\frac{1}{\rho}\frac{\partial p}{\partial z} + g. \qquad (7)$$

If the long waves (tidal motion) are considered, it is usual to neglect $\partial w/\partial t$. Thus the equation of motion in the z-direction can be considerably simplified to:

$$0 = -\frac{1}{\rho}\frac{\partial p}{\partial z} + g, \quad \text{or} \quad \frac{\partial p}{\partial z} = \rho g.$$

When ρ is constant (as it is in our case) then by simple integration we obtain for a homogeneous sea;

$$p = \rho g z + f(x, y, t) \tag{8}$$

Taking into account the boundary conditions on the sea surface (regarded as horizontal), remembering that at the surface the water pressure is equal to the atmospheric pressure $p = p_a$ (denoting by p_a the atmospheric pressure $p_a(x,y,t)$) we obtain from (8)

$$p = p_a + \rho g (z + \zeta); \tag{9}$$

where ζ is the elevation of the sea surface, i.e. disturbance in height of the free surface from its undisturbed level.

Equation (9) corresponds to the basic hydrostatic equation, this means that the pressure at any depth is given by the hydrostatic law for pressure.

Coming back to the remaining two equations of motion (5) and (6) the pressure gradient terms can now be expressed (by differentiating equation (9)) in terms of atmospheric pressure and surface slope. Simply speaking, the derivatives of the pressure (in the horizontal directions) now become functions of the water level and the atmospheric pressure:

$$\frac{\partial p}{\partial x} = \frac{\partial p_a}{\partial x} + \frac{\partial}{\partial x}\left[\rho g (z+\zeta)\right] = \frac{\partial p_a}{\partial x} + \rho g \frac{\partial \zeta}{\partial x},$$

$$\frac{\partial p}{\partial y} = \frac{\partial p_a}{\partial y} + \frac{\partial}{\partial y}\left[\rho g (z+\zeta)\right] = \frac{\partial p_a}{\partial y} + \rho g \frac{\partial \zeta}{\partial y}.$$

Substituting these into the first equations of motion (5) and (6) we obtain:

$$\frac{\partial u}{\partial t} = fv - g\frac{\partial \zeta}{\partial x} - \frac{1}{\rho}\frac{\partial p_a}{\partial x} - \frac{1}{\rho}\frac{\partial F}{\partial z}, \tag{10}$$

$$\frac{\partial v}{\partial t} = -fu - g\frac{\partial \zeta}{\partial y} - \frac{1}{\rho}\frac{\partial p_a}{\partial y} - \frac{1}{\rho}\frac{\partial G}{\partial z}. \tag{11}$$

The above equations, since we are not taking into account the atmospheric effect on the sea surface, can be further simplified and written as:

$$\frac{\partial u}{\partial t} - fv = -g\frac{\partial \zeta}{\partial x} - \frac{1}{\rho}\frac{\partial F}{\partial z}, \tag{12}$$

$$\frac{\partial v}{\partial t} + fu = -g\frac{\partial \zeta}{\partial y} - \frac{1}{\rho}\frac{\partial G}{\partial z}, \tag{13}$$

and repeating the equation

$$\frac{\partial u}{\partial x} + \frac{\partial v}{\partial y} + \frac{\partial w}{\partial z} = 0 \tag{14}$$

we obtained the whole set of hydrodynamic-differential equations, of motion and continuity, needed as a starting point to establish our fundamental prediction equations.

The next step is to integrate the primitive equations (12), (13) and (14) from the bottom to the surface.

The technique of such integration has been discussed by Proudman (1953), Welander (1961) and Ueno (1964). According to this integration a set of equations is obtained which is independent of the vertical co-ordinate.

Integrating the whole set of equations from the bottom to the surface and introducing the surface, and especially the bottom boundary conditions, we obtain the resultant set of equations, which govern the motion in the sea, in the following form:

$$\frac{\partial U}{\partial t} - fV = -g(h+\zeta)\frac{\partial \zeta}{\partial x} + \frac{1}{\rho}(F_s - F_b), \tag{15}$$

$$\frac{\partial V}{\partial t} + fU = -g(h+\zeta)\frac{\partial \zeta}{\partial y} + \frac{1}{\rho}(G_s - G_b), \tag{16}$$

and

$$\frac{\partial \zeta}{\partial t} = -\frac{\partial U}{\partial x} - \frac{\partial V}{\partial y}; \tag{17}$$

where:

$$U = \int_{z=-\zeta}^{z=h} u\,dz \quad \text{and} \quad V = \int_{z=-\zeta}^{z=h} v\,dz. \tag{18}$$

The wind stress components, F_s and G_s in the x and y directions respectively, occur in the equations as a result of the surface boundary conditions;

$$-\mu \frac{\partial u}{\partial z} = F_s \quad \text{and} \quad -\mu \frac{\partial v}{\partial z} = G_s \quad (\text{at } z=0), \tag{19}$$

where: μ is the coefficient of eddy viscosity, generally assumed for theoretical purposes to be constant.

Correspondingly we can write the conditions at the sea bottom:

$$-\mu \frac{\partial u}{\partial z} = F_b \quad \text{and} \quad -\mu \frac{\partial v}{\partial z} = G_s \quad (\text{at } z=h), \tag{20}$$

where: F_b and G_b express the components of the bottom friction in terms of bottom current. According to Welander (1957) the alternative bottom condition is:

$$u = v = 0 \qquad (\text{at } z = h). \tag{21}$$

Due to the fact that in this study tidal problems only are considered, the surface stresses of the wind effect are ignored and only the bottom friction is taken into account.

It is assumed here that the resultant bottom stress, according to the recognised quadratic law, will be given in components of the total stream by:

$$F_b = \frac{k_b \rho U \sqrt{U^2+V^2}}{(h+\zeta)^2}, \tag{22}$$

$$G_b = \frac{k_b \rho V \sqrt{U^2+V^2}}{(h+\zeta)^2}; \tag{23}$$

where k_b is the coefficient of bottom friction (varying value as will be shown later), taken according to Proudman (1953), and others as 0·0025; for the parent model only.

Taking into account all the aforementioned assumptions and restrictions the final hydrodynamic differential equations, with the above defined bottom stress components, can be expressed as:

$$\frac{\partial U}{\partial t} = fV - g(h+\zeta)\frac{\partial \zeta}{\partial x} - k_b \frac{U\sqrt{U^2+V^2}}{(h+\zeta)^2}, \tag{24}$$

$$\frac{\partial V}{\partial t} = -fU - g(h+\zeta)\frac{\partial \zeta}{\partial y} - k_b \frac{V\sqrt{U^2+V^2}}{(h+\zeta)^2}, \tag{25}$$

$$\frac{\partial \zeta}{\partial t} = -\frac{\partial U}{\partial x} - \frac{\partial V}{\partial y}. \tag{26}$$

7·2 Initial and boundary conditions

In addition to the mentioned surface and bottom conditions, initial and lateral boundary conditions of the elevation and stream flow are required in order to solve the previously derived equations (24), (25) and (26).

Here, as the study considers tidal problems only, the initial conditions of the astronomical tide have to be specified. Thus at time t = 0 the values of U(x,y,t), V(x,y,t) and, in our case, the elevation value ζ(x,y,t) have to be described. Also at land boundaries and at the artificial boundaries, located across the open sea areas and called open boundaries, boundary conditions are required for all the time.

It should be mentioned that the component of the flow normal to the land boundary is permanently zero:

$$U \cos \varphi + V \sin \varphi = 0,$$

where φ is the angle between normal to the coast line and the x-axis (figure 4).

It follows that:

U = 0, is the boundary condition for the stream points on the land boundaries lying along parallels of the y-axis;

V = 0, is the boundary condition for the stream points on the land boundaries lying along parallels of the x-axis.

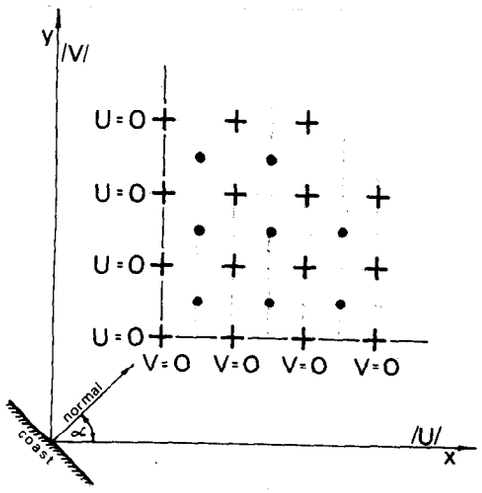

Figure 4. Definition of normal flow.

Elevation along the open boundaries is either assumed to be permanently zero or specified as a function of time and position. The former condition is most suitable for deep water open boundaries where the elevation is generally small, but for shallow waters considered in this study the second condition has to be applied.

The existing co-tidal charts (e.g. see the one prepared in figure 2) enable us to specify, one supposes with sufficient accuracy, the elevation as a function of time and position along the open boundary of the model sea.

7·3 The array of grid points

The choice of a grid net and the grid size is usually based on the accuracy required and, moreover, on the type of computer to be used.

Three arrays of grid nets were prepared for the eastern part of the Irish Sea. They included three cases: parent model without barriers and parent model with barrage alignments, in Morecambe Bay and the Solway Firth. One of the prepared matrices is shown in figure 5.

The meshes of any of the parent models were selected in such a way that the grid nets for the small models could have the x, y axes parallel and perpendicular to the main (longitudinal) axis of the concerned estuary.

Figure 5 consists of two different sets of grid points: dots for elevation values (ζ) and crosses for stream values; U, along x-axis and V along y-axis respectively.

The basis for selecting a proper mesh is the classical Courant-Friedrich-Lewy (1928) criterion, which governs the numerical stability of a two-dimensional finite-difference scheme.

For a square mesh, as chosen in this work, the necessary condition for stability is the fulfilment of the following inequality:

$$\Delta t \leqslant \frac{2}{\sqrt{gh}} \Delta s$$

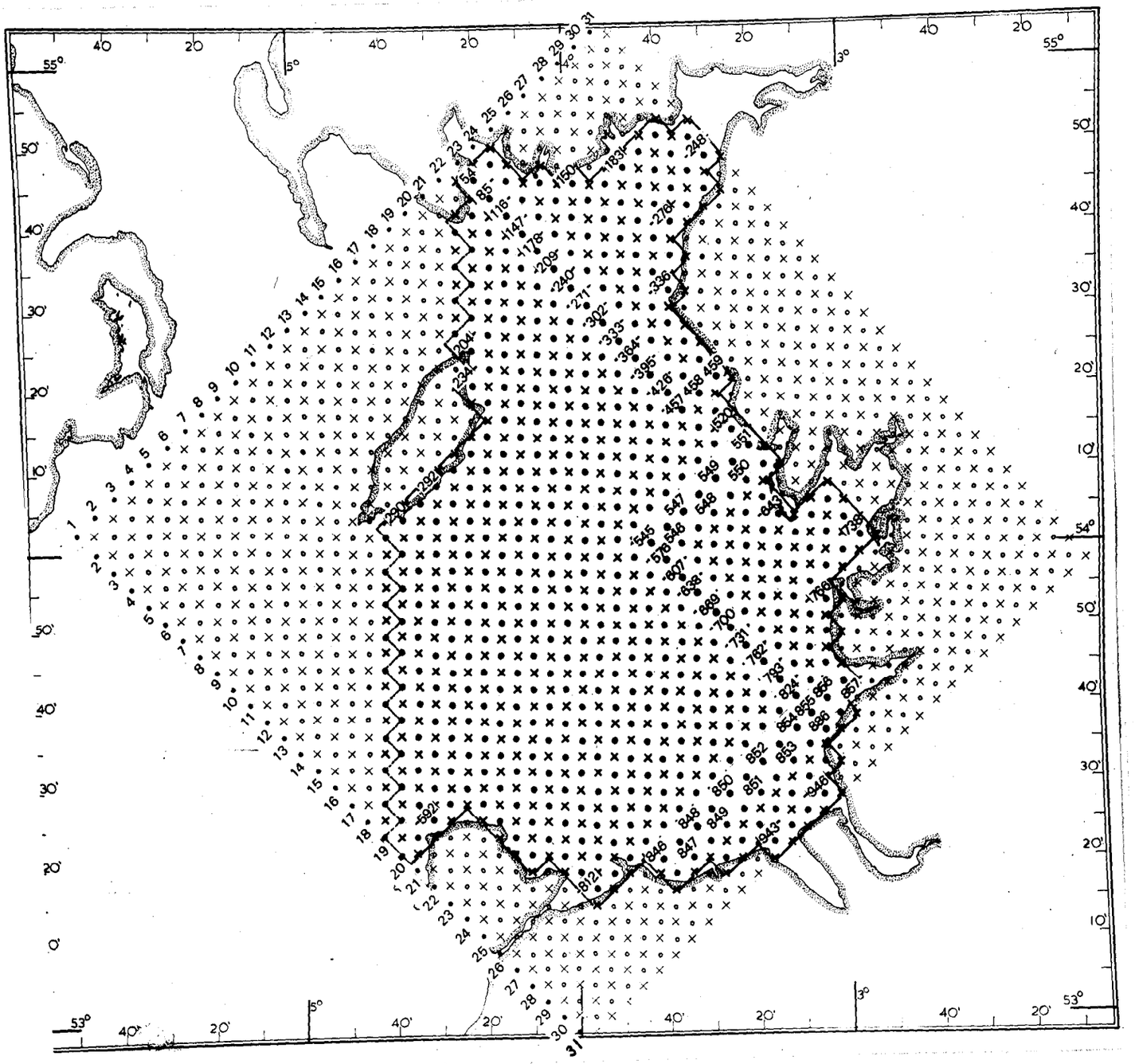

Figure 5. Finite-difference grid for the eastern part of the Irish Sea. Numbers at various places (at elevation points) indicate the seeking elevation values at the open boundaries for the small models and elevation values for some of the coastal stations.

which shows an explicit dependence between the values of the spacial increments, namely the mesh width value Δs (cm) and time increments Δt (sec). Neglecting this rule the expected convergence of the computed solutions to the real solution of the difference equations may not occur but rather a 'blow-up' of the computational values might be experienced.

Theoretical analyses to difference procedures show that, for a system to be numerically stable, the grid size and timestep cannot be chosen indepently.

According to the criterion the following values, of Δs ($\Delta x = \Delta y = \Delta s$) and Δt, for the parent model were chosen: Δs = 2781 m and Δt = 120 sec.

The real land boundary is represented by a step-like boundary, so that the mesh chosen reproduces the coastline with sufficient accuracy. The same conditions were applied to the small estuarial models.

7·4 Labelling system and indication of grid points

The meshes, covering the considered water areas of all models in discussion, consist of 2p horizontals, numbered serially 1,2,3,4.... downwards through the grid. Each horizontal has n grid points of elevation and stream. All the grid points have, as is shown below, their own co-ordinate designation constituting interlacing submeshes, figure 6.

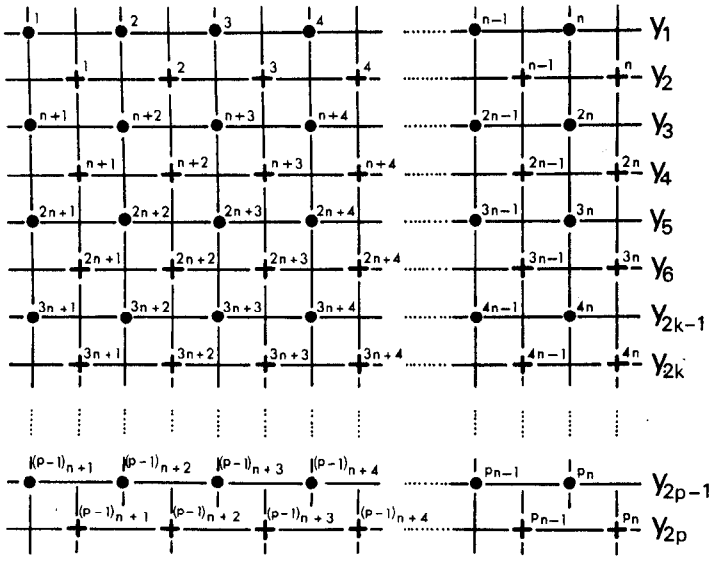

Figure 6. Labelling system of the grid points.

The horizontals, of the elevation sub-mesh, are labelled j = 1,3,5,... ..2_{k-1}, ... 2_{p-1}, and in the stream sub-mesh as j = 2,4,6,... 2_k, ... 2_p. A serial numbering for the grid points, at both sub-meshes, is applied and

runs from left to right along alternate horizontals moving downwards across the whole grid. Apparently any elevation or stream point i is associated with particular j showing the horizontal on which the point is located. A single suffix notation of the integer i will be given to each elevation or stream point, denoting the value ζ at elevation point i by ζ_i. The same applied to stream values $U = U_i$ and $V = V_i$ at points fixed by appropriate integer i. Such notation facilitates the programming for numerical calculations.

The horizontal and vertical lines (latitude and longitude) build a rectangular matrix of points which encloses the real matrix of the sea. It is obvious that all fictitious grid points within the rectangular frame, but outside the sea area must be labelled as well. The fictitious points will not take any real part in the calculations but will enable us to obtain the output values in a configuration resembling the natural sea under consideration.

A set of rectangular matrices, for the 4 models considered, was prepared giving the following dimensions: (but for no barrier cases only, for other arrays were prepared when a barrage crossing was introduced)

(a) 34 x 31 squares (1054 elevation and 1054 stream points) for the parent model,

(b) 35 x 42 squares (1470 elevation and 1470 stream points) for Solway Firth model,

(c) 29 x 34 squares (986 elevation and 986 stream points) for Morecambe Bay model, and

(d) 39 x 60 squares (2340 elevation and 2340 stream points) for River Dee model.

Figure 7 gives the indication of various categories of points on a fictitious sea region.

Applying this notation to our real sea model all the different types of grid point location, denoted by integer 1 to 14 respectively can be found.

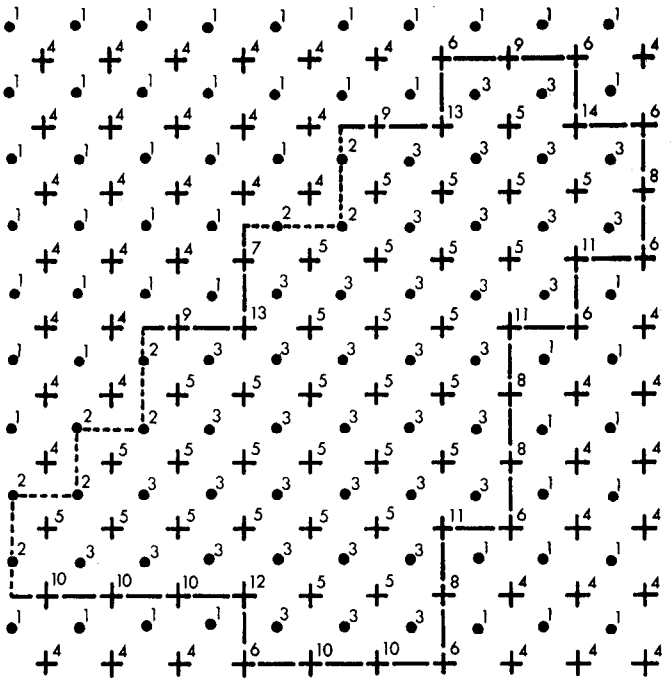

Figure 7. Indication of various categories of points.

To explain the above given figure, namely, all the various categories of grid points and their appropriate integer label i, the following description comprising different elevation and stream points is set out:

label '1' - denotes the elevation point i, located outside the model boundary

" '2' - ... on the open boundary,

" '3' - ... within the boundary.

" '4' - denotes the stream point i, located outside the model boundary,

" '5' - ... within the boundary,

" '6' - ... at a 90° corner of the boundary,

" '7' - ... on the longitudinal section of the boundary,

" '8' - ... as above,

" '9' - ... on the latitudinal section of the boundary,

" '10' - ... as above,

" '11' - ... at a 270° corner of the boundary,

" '12' - ... as above,

" '13' - ... as above,

" '14' - ... as above.

7·5 The transformation of the hydrodynamic-differential equations into finite differences

A numerical solution of the established hydrodynamic-differential equations (24), (25) and (26) can be achieved by approximating the differential quotients to finite differences in space and time co-ordinates at definite points of a grid system. Various ways exist of representing differential equations in finite-difference form.

The space derivatives, in our hydrodynamical equations, are expressed as central differences. For time derivaties, in the equations of motion, forward differences were used. To maintain stability of the numerical solution the time derivatives in the equation of continuity are described by backward differences.

It follows, from the above, that values of the variables U_i, V_i and ζ_i at time $(m + 1)\Delta t$, and lying within the sea, are derived from the values at the preceding time $m\Delta t$. Here Δt is the time interval between successive computations, and m is an integer.

Returning to the differential equations we can now replace the equation of continuity (26) at an elevation point i, lying within the sea, by the following finite-difference equation:

$$\frac{\zeta_{m+1,i} - \zeta_{m,i}}{\Delta t} = - \frac{B_{m+1,i}}{2\Delta x} - \frac{C_{m+1,i}}{2\Delta y} ; \qquad (27)$$

where the quotients $B_i/2\Delta x$ and $C_i/2\Delta y$ represent the derivatives $\partial U/\partial x$ and $\partial V/\partial y$ in equation (26).

The values of B_i and C_i are expressed as

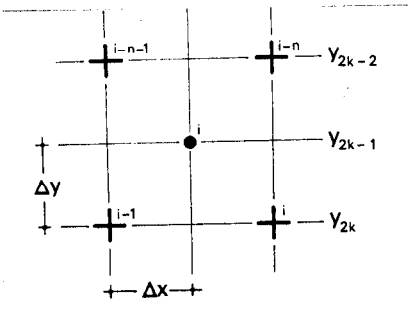

Figure 8

$$B_i = \frac{1}{2}(U_{i-n} - U_{i-n-1} + U_i - U_{i-1}),$$

$$C_i = \frac{1}{2}(V_{i-n} - V_i + V_{i-n-1} - V_{i-1}), \qquad (28)$$

and are the averaged central differences formed from the values of U and V at four stream points surrounding the elevation point i, Figure 8.

Now replacing the differential equations of motion (24) and (25) by finite-differences we obtain:

$$\frac{U_{m+1,i}-U_{m,i}}{\Delta t}=fV_{m,i}-g(h_i+Z_{m,i})\frac{D_{m,i}}{2\Delta x}-k_b\frac{U_{m,i}\left|\sqrt{U_{m,i}^2+V_{m,i}^2}\right|}{(h_i+Z_{m,i})^2} \tag{29}$$

$$\frac{V_{m+1,i}-V_{m,i}}{\Delta t}=-fU_{m,i}-g(h_i+Z_{m,i})\frac{E_{m,i}}{2\Delta y}-k_b\frac{V_{m,i}\left|\sqrt{U_{m,i}^2+V_{m,i}^2}\right|}{(h_i+Z_{m,i})^2} \tag{30}$$

The derivatives $\partial\zeta/\partial x$ and $\partial\zeta/\partial y$ are replaced by finite differences $D_i/2\Delta x$ and $E_i/2\Delta y$. The $Z_{m,i}$ value represents the elevation at astream point i at time $m\Delta t$.

Rearranging the equations (27), (29) and (30) into:

$$U_{m+1,i}=U_{m,i}\left[1-k_b\frac{\left|\sqrt{U_{m,i}^2+V_{m,i}^2}\right|}{(h_i+Z_{m,i})^2}\Delta t\right]+fV_{m,i}\Delta t-g(h_i+Z_{m,i})\frac{D_{m,i}}{2\Delta x}\Delta t, \tag{31}$$

$$V_{m+1,i}=V_{m,i}\left[1-k_b\frac{\left|\sqrt{U_{m,i}^2+V_{m,i}^2}\right|}{(h_i+Z_{m,i})^2}\Delta t\right]-fU_{m,i}\Delta t-g(h_i+Z_{m,i})\frac{E_{m,i}}{2\Delta y}\Delta t, \tag{32}$$

and

$$\zeta_{m+1,i}=\zeta_{m,i}-\frac{B_{m+1,i}}{2\Delta x}\Delta t-\frac{C_{m+1,i}}{2\Delta y}\Delta t, \tag{33}$$

we obtain the stream flows at time $(m+1)\Delta t$, where the suffix i refers to a stream print of latitude y_{2k}.

The forms taken by D_i, E_i and Z_i, as will become apparent, vary according to the position of the stream point i relative to the land boundary.

At a stream point i, lying on a longitudinal land boundary as shown in Figure 9a and 9b.

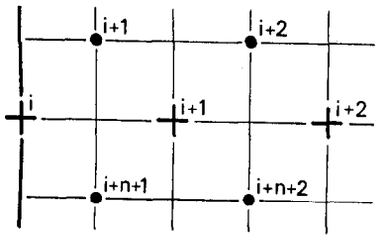

Figure 9a

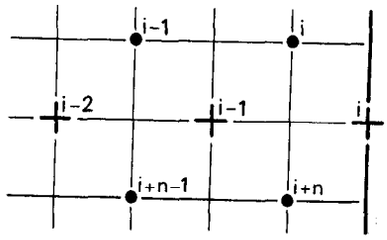

Figure 9b

where the value of U_i (according to our boundary condition §7.2) is permanently zero, the stream flow is

$$V_{m+1,i} = V_{m,i}\left[1 - k_b \frac{|V_{m,i}|}{(h_i + Z_{m,i})^2}\Delta t\right] - g(h_i + Z_{m,i})\frac{E_{m,i}}{2\Delta y}\Delta t. \qquad (34)$$

Similarly at a stream point i, on a latitudinal land boundary, as shown in Figure 10a and 10b

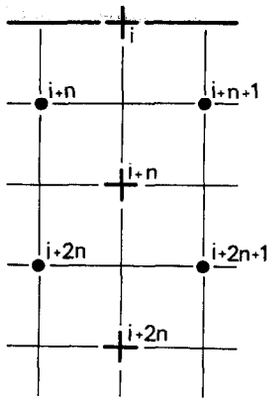

Figure 10a

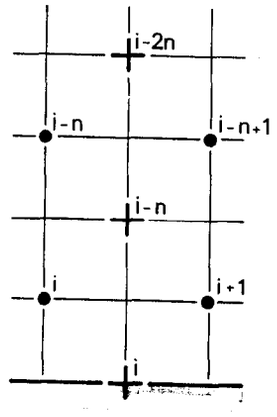

Figure 10b

where now the V_i value is permanently zero, the stream flow is

$$U_{m+1,i} = U_{m,i}\left[1 - k_b \frac{|U_{m,i}|}{(h_i + Z_{m,i})^2}\Delta t\right] - g(h_i + Z_{m,i})\frac{D_{m,i}}{2\Delta x}\Delta t. \qquad (35)$$

7·5·1 The value of elevation Z at a stream point i

The value of Z_i depends, as it was said already, on the location of the stream point i.

At a stream point i, lying within the model boundary, as in Figure 11, the value of Z_i is an average of the elevations surrounding the point.

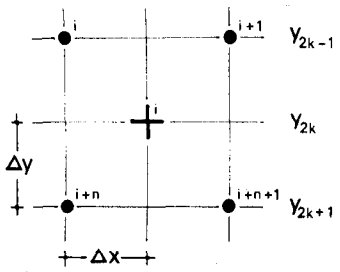

$$Z_i = \frac{1}{4}\left(\zeta_i + \zeta_{i+1} + \zeta_{i+n} + \zeta_{i+n+1}\right). \qquad (36)$$

Figure 11

In estimating the Z_i values at different locations let us consider the following Figures 12a and 12b

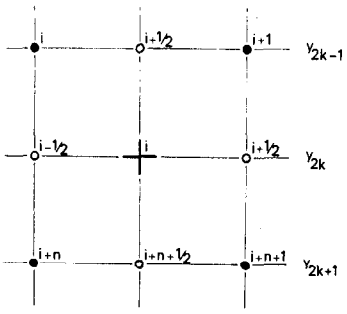

Figure 12a

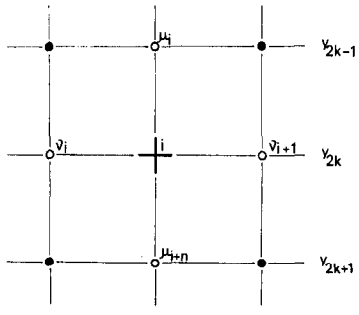

Figure 12b

Figures 12a and 12b show our fictitious points surrounding the stream point i where the elevation will be denoted by:

(a) μ_i - for the point due north of i, labelled $i + \frac{1}{2}$, 2_{k-1}, since it lies between elevation points i and i + 1 on parallel 2_{k-1} north of the stream point i.

(b) μ_{i+n} - for the point due south of i, labelled $i+n+\frac{1}{2}$, 2_{k+1}, since it lies between elevation points i+n and i+n+1 on parallel 2_{k+1}, south of stream point i.

(c) ϑ_i - for the point due west of i, labelled $i-\frac{1}{2}$, 2_k, since it lies between points i-1 and i.

(d) ϑ_{i+1} - for the point due east of i, labelled $i+\frac{1}{2}$, 2_k, since it lies between points i and i+1 on the same parallel as i.

The above scheme (Banks, 1967) will enable us to describe the elevations and elevation gradients at different land boundaries.

Applying three point Lagrange extrapolations from the elevations adjacent to the boundaries, we obtain μ_i and ν_i as given below.

When the land is to the west of the boundary as in Figure 9a;

$$\mu_i = \frac{1}{2}(3\zeta_{i+1} - \zeta_{i+2}). \tag{37}$$

When the land is to the east of the boundary, as in Figure 9b;

$$\mu_i = \frac{1}{2}(3\zeta_i - \zeta_{i-1}). \tag{38}$$

When the land is to the north of the boundary, as in Figure 10a;

$$\nu_i = \frac{1}{2}(3\zeta_{i+n} - \zeta_{i+2n}). \tag{39}$$

When the land is to the south of the boundary, as in Figure 10b;

$$\nu_i = \frac{1}{2}(3\zeta_i - \zeta_{i-n}). \tag{40}$$

The elevation at a stream point i lying on a longitude boundary (Figures 9a and 9b), will be given by:

$$Z_i = \frac{1}{2}(\mu_i + \mu_{i+n}), \tag{41}$$

being the average of the elevation values, at the fictitious points, due north and south of point i.

In the same way we derive the elevation of any stream point i lying on a latitude boundary (Figures 10a and 10b) by forming:

$$Z_i = \frac{1}{2}(\nu_i + \nu_{i+1}), \tag{42}$$

that is by averaging the elevations at assumed points due east and west of the stream point i. It follows that at any stream point i lying at a corner formed by a 90° sector of coast, as in Figure 13(a,b,c,d,), the elevation Z_i can be taken as an average of Z's given above.

Thus,

$$Z_i = \frac{1}{4}(\mu_i + \mu_{i+n} + \nu_i + \nu_{i+1}), \tag{43}$$

where the values of μ and ν are appropriate to the type of longitude and latitude boundaries forming the corner.

The following Figure 13, shows various corner points with coast in different quadrants:

(a) coast in the quadrant south to east;

(b) coast in the quadrant south to west;

(c) coast in the quadrant north to east;

(d) coast in the quadrant north to west.

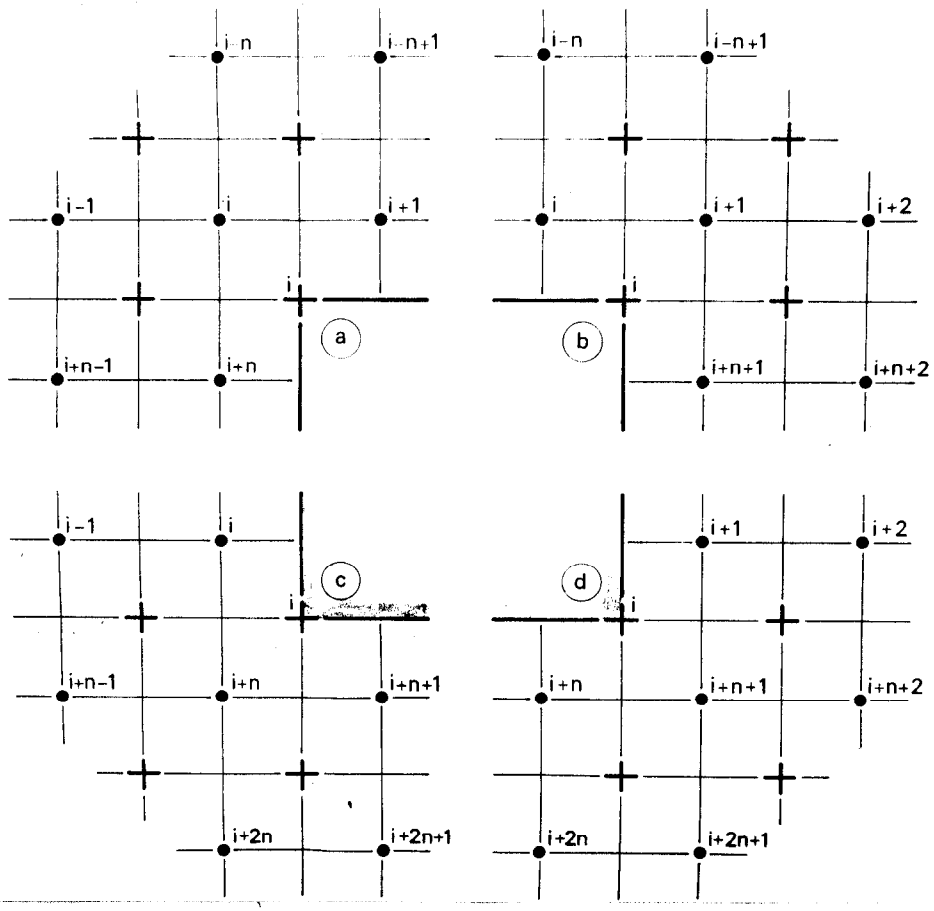

Figure 13

In this way we can express the elevation Z_i at the 90° corner, with coast in the quadrant south to east (Figure 13a) as

$$Z_i = \frac{1}{8}\left[6\zeta_i + 3(\zeta_{i+1} + \zeta_{i+n}) - (\zeta_{i-n} + \zeta_{i-n+1} + \zeta_{i-1} + \zeta_{i+n-1})\right]. \quad (43a)$$

which is obtained by substituting μ_i and ν_i from equations (38) and (40), respectively, into equation (43).

Similarly at stream point i, at a corner with coast in the quadrant south to west (Figure 13b), as

$$Z_i = \frac{1}{8}\left[6\,\zeta_{i+1} + 3(\zeta_i + \zeta_{i+n+1}) - (\zeta_{i-n} + \zeta_{i-n+1} + \zeta_{i+2} + \zeta_{i+n+2})\right]. \qquad (43b)$$

In the same way for stream point i, at a corner with coast in the quadrant north to east (Figure 13c), the elevation value Z_i at point i is given by

$$Z_i = \frac{1}{8}\left[6\,\zeta_{i+n} + 3(\zeta_i + \zeta_{i+n+1}) - (\zeta_{i-1} + \zeta_{i+n-1} + \zeta_{i+2n+1} + \zeta_{i+2n})\right]. \qquad (43c)$$

Again for a stream point i, at a corner with coast in the quadrant north to west (Figure 13d)

$$Z_i = \frac{1}{8}\left[6\,\zeta_{i+n+1} + 3(\zeta_{i+1} + \zeta_{i+n}) - (\zeta_{i+2} + \zeta_{i+n+2} + \zeta_{i+2n} + \zeta_{i+2n+1})\right]. \qquad (43d)$$

7·5·2 The surface gradients at a stream point i

The surface gradients represented in the finite-difference equations, and denoted by D_i and E_i, are now discussed briefly.

For the sake of convenience let us repeat the figure with a stream point i lying within the model boundary (Figure 14)

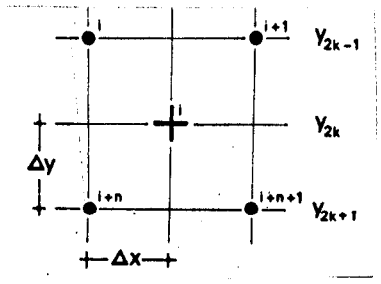

Figure 14

The gradients of elevation for an interior point i, as in Figure 14, are expressed by

$$D_i = \frac{1}{2}(\zeta_{i+n+1} - \zeta_{i+n} + \zeta_{i+1} - \zeta_i), \qquad (44)$$

$$E_i = \frac{1}{2}(\zeta_i - \zeta_{i+n} + \zeta_{i+1} - \zeta_{i+n+1}). \qquad (45)$$

The elevation gradient for a stream point i, lying on a longitude coastal boundary (Figures 9a and 9b), where according to our assumed boundary condition $U_i = 0$ for all the time:

$$E_i = \zeta_i - \zeta_{i+n}. \qquad (46)$$

Similarly for stream point i, lying on a latitude land boundary (Figures 10a and 10b) where again $V_i = 0$ is permanently zero

$$D_i = \nu_{i+1} - \nu_i \,. \tag{47}$$

Applying the same reasoning to astream point i, at a corner point formed by 90° sector of land (Figure 13) where the values of μ_i and ν_i are defined by equations (37), (38), (39) and (40) yields

$$E_i = \mu_i - \mu_{i+n}, \tag{48}$$

$$D_i = \nu_{i+1} - \nu_i \,. \tag{49}$$

Thus, a stream point i, at a corner with coast in the south-east quadrant (Figure 13a) can be taken as:

$$E_i = \frac{1}{2}(3\zeta_i - \zeta_{i-1} - 3\zeta_{i+n} + \zeta_{i+n-1}), \tag{50}$$

$$D_i = \frac{1}{2}(3\zeta_{i+1} - \zeta_{i-n+1} - 3\zeta_i + \zeta_{i-n}), \tag{51}$$

where the values of $_i$ in equation (38) and $_i$ in equation (40) are applied.

Considering the remaining stream point i, lying in the three different corners, we obtain:

for a corner with land in the wouth-west quadrant (Figure 13b) using equation (38) and (40)

$$E_i = \frac{1}{2}(3\zeta_{i+1} - \zeta_{i+2} - 3\zeta_{i+n+1} + \zeta_{i+n+2}), \tag{52}$$

$$D_i = \frac{1}{2}(3\zeta_{i+1} - \zeta_{i-n+1} - 3\zeta_i + \zeta_{i-n}), \tag{53}$$

for a corner with land in the north-east quadrant (Figure 13c), using equation (38) and (39)

$$E_i = \frac{1}{2}(3\zeta_i - \zeta_{i-1} - 3\zeta_{i+n} + \zeta_{i+n-1}), \tag{54}$$

$$D_i = \frac{1}{2}(3\zeta_{i+n+1} - \zeta_{i+2n+1} - 3\zeta_{i+n} + \zeta_{i+2n}), \tag{55}$$

for a corner with land in the north-west quadrant (Figure 13d), using equation (37) and (39)

$$E_i = \frac{1}{2}(3\zeta_{i+1} - \zeta_{i+2} - 3\zeta_{i+n+1} + \zeta_{i+n+2}), \quad (56)$$

$$D_i = \frac{1}{2}(3\zeta_{i+n+1} - \zeta_{i+2n+1} - 3\zeta_{i+n} + \zeta_{i+2n}). \quad (57)$$

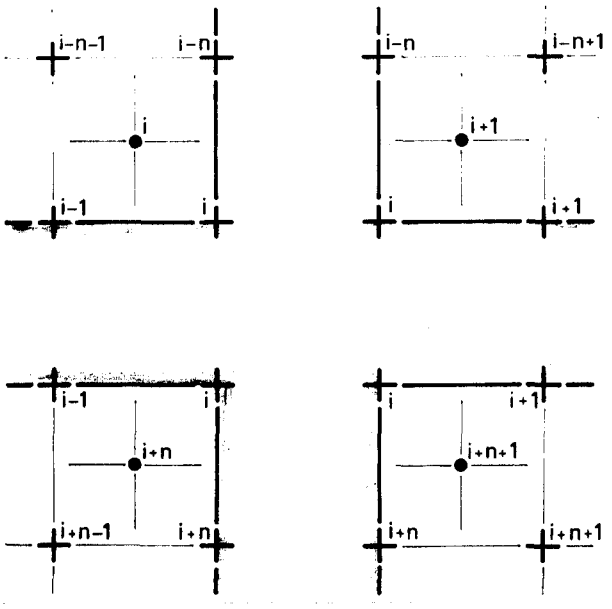

Figure 15. Sea area in different quadrants formed by 270° sector of coast.

According to the previously assumed boundary condition it is apparent that for a stream point i, lying at a corner formed by 270° sector of coast, as in the enclosed figure 15, the values for U_i and V_i are zero all the time.

8. The data

Besides the formulation of the equations, the appropriate grid and mesh system, labelling designation and the programming technique, a set of hydrographic and general initial data is required to commence the numerical calculations.

A layout, and short description of these data,now follows

8·1 Depth values

A set of depth values has been prepared from relevant charts and read firstly as average values surrounding an elevation point. The real depths were read finally at a stream point as an average value from the four elevation points adjacent to that point. Such a method gives the necessary smoothing required for numerical analysis.

Figure 16 gives the depth distribution(in cm) at any stream point i for the eastern area of the Irish Sea lying within or on the boundary but not at

a corner formed by 270° sector of coast.

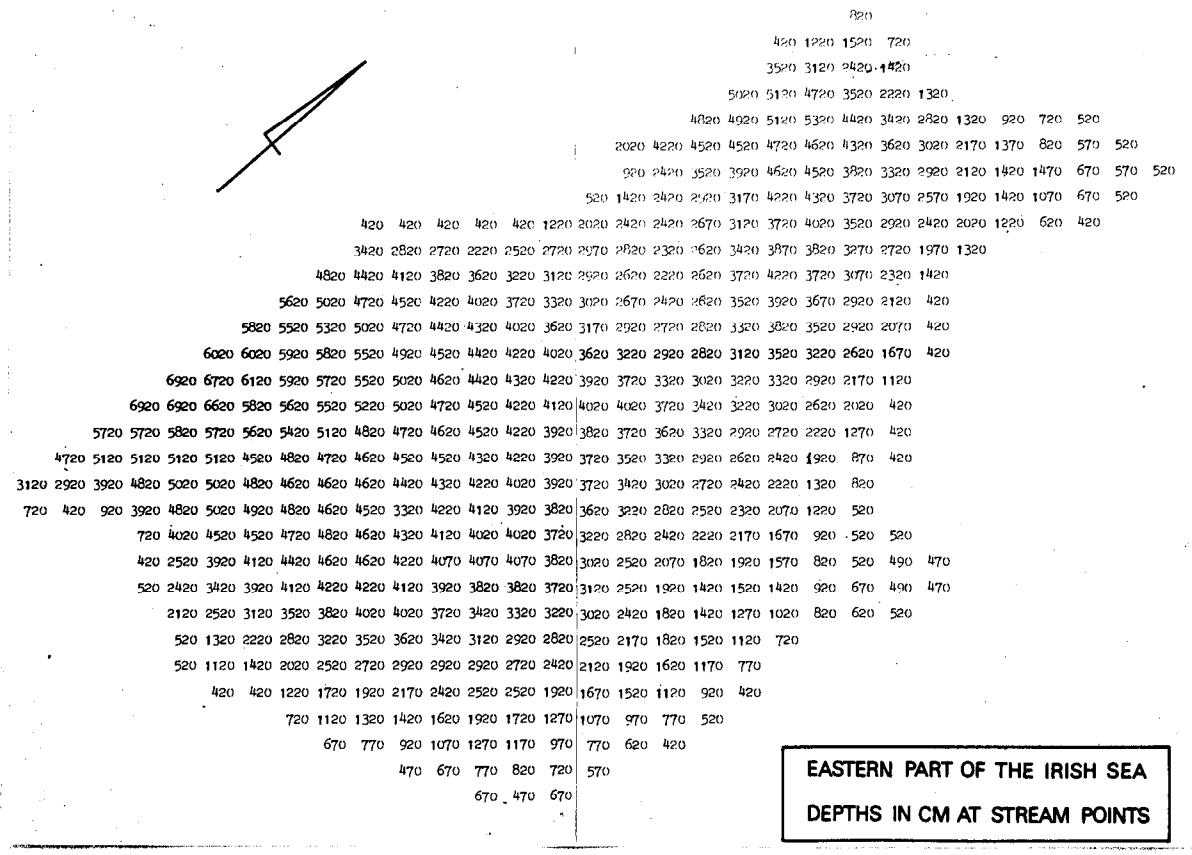

Figure 16. Depth distribution in the eastern part of the Irish Sea.

8·2 Open boundary input

Figure 17 shows the H (cm) and g (deg) parameters of the M_2 constituent taken as initial tidal data for the parent model investigations.

The values were interpolated from the co-tidal chart (Figure 2) and read at the 27 elevation points which build up the open boundary of the numerical model. The M_2 tide specified at those points gives the 'feeding' values enabling us to generate the M_2 wave in the model sea.

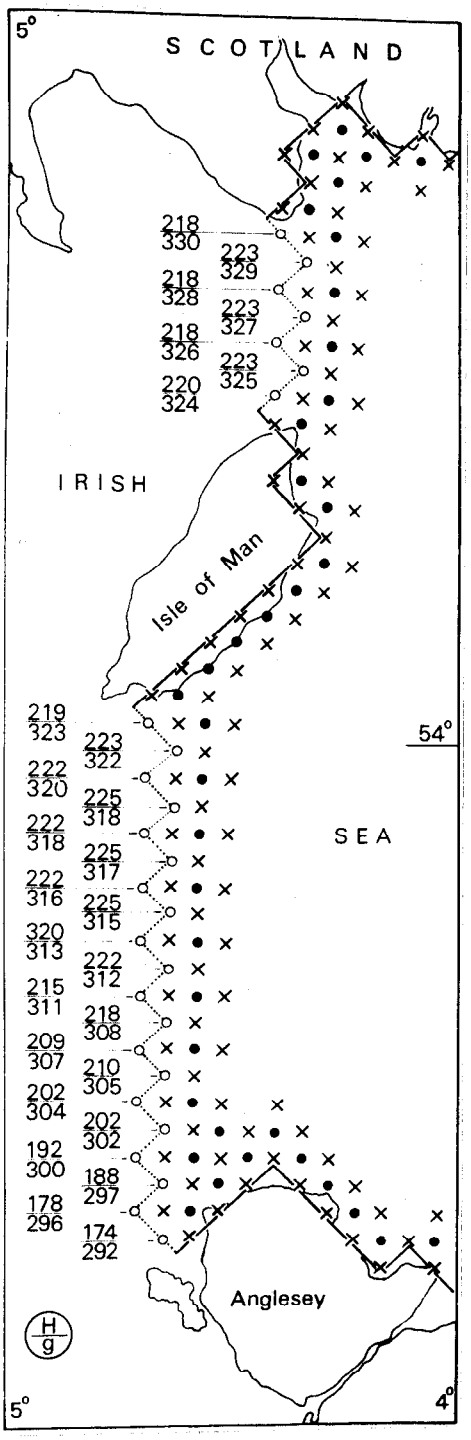

Figure 17. Amplitudes (H) and phases (g) of the M_2 tide at the open boundary of the parent model.

8·3 Constant values

All the constants, needed for the calculations, were taken in CGS units giving in result, for the four models considered, the following values:

(a) Parent model: Δs = 278100 cm; Δt = 120 sec; h_{max} = 6920 cm;

ρ = 1·0 g.cm^{-3}; k_b = 0·0025; g = 981 cm.sec^{-2}

f = 0·0001175 sec^{-1}; j (speed of constituent) = 0·008333;

(b) Morecamby Bay; Δs = 92700; Δt = 90; h_{max} = 3450; f = 0·0001175

The other values as in (a); apart from value k_b

'Discussion' on k_b parameter is given in § 10.

(c) Solway Firth ; Δs = 92700; Δt = 60; h_{max} = 4700; f = 0·0001181

(d) River Dee; Δs = 46350; Δt = 40; h_{max} = 2500; f = 0·0001163.

9. Evaluation of currents and elevations

It is impossible to discuss in detail the whole procedure of obtaining the seeking values, i.e. elevations and currents, therefore the following short description of the calculating technique follows only.

Before commencing the calculations all values of , U and V have to be specified at appropriate grid points, of the model sea, at the time mΔt, or the elevations along the open boundaries has to be given as a function of time. As mentioned in the preceding paragraph the latter condition was applied. Thus, the values of elevation (ζ) in the form of harmonic constants (H) and (g) were described at the starting point (t=0) of our calculations.

Applying the equations (31), (32) and the devised formulae, relevant to the locations of the different points, i.e. the various equations for $Z_{m,i}$, $D_{m,i}$ and $E_{m,i}$, stream flow values of U_{m+1i} and $V_{m+1,i}$ for each stream point i of the model were obtained.

The elevation value $Z_{m,i}$ at any stream point i was obtained from the equation relevant to the location of such a point i (see § 7·5·1). With the help of the $Z_{m,i}$ value obtained the depth mean velocities $U_i/(h_i+Z_i)$ and $V_i/(h_i+Z_i)$ were determined at time mΔt.

Continuity equation (33) together with the appropriate equations for B_i and C_i, yielded $_{m+1,i}$ for any elevation point i.

The enclosed figure 18 (Heaps 1969) shows the flow diagram of the iterative procedure how the required values of U_i, V_i, D_i, E_i at each stream point i, within or on the model boundaries, and the values of ζ_i and B_i, C_i, at each elevation point i, within the model sea, were calculated.

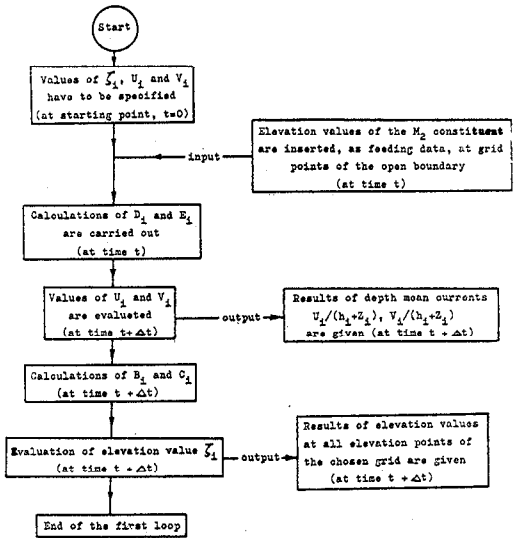

Figure 18. Flow diagram showing the evaluation of the required values: U_i, V_i, D_i, E_i at each stream point i, and ζ_i, B_i, C_i at each elevation point i, of the model sea.

The figure represents one loop of the iterative procedure. The calculation proceeds by applying the loop for many successive time steps, say, $t = 0$, Δt, $2\Delta t$, $3\Delta t$ ... etc., up to $(m-1)\Delta t$. Thus, by consecutive iterations (depending on the time step chosen) the displacement of ζ_i, U_i, V_i values, in the sea of interest, is given numerically.

9·1 Program and computer used

The programming technique for ordering the whole set of calculations was based on a scheme devised by Banks (1967). The computer program, for the calculating procedure was written in ALGOL and all the runs were carried out on an English Electric KDF9 with a 32K computer core memory.

The order of calculations and printing out of the results was facilitated by designating to each grid point of the sea region an integer label of the group to which the point i belongs (see § 7·4)

Each run of the program simulates the elevations (ζ) and depth mean currents $U/(h+\zeta)$, $V/(h+\zeta)$, induced in the model sea by the open boundary values.

The output values, given in a shape of the basin considered, were obtained according to the data prescribed. The last values, of each run, were generally stored on magnetic tapes enabling further calculations to be carried out if unsatisfactory results were obtained.

A layout of the computer program (Z621100) used to carry out all the calculations in discussion is enclosed in Appendix I.

10. Calculations and the results

Many calculations have been carried out to reproduce the M_2 tide in the eastern part of the Irish Sea and its estuaries.

Some difficulties were encountered in these runs which necessitated a modification to the program to deal with the shallow water areas. The non-linear depth term $(h+\zeta)$ was replaced by $(h+\alpha\zeta)$, where the parameter α was initially taken to be zero then increased to 0·2, 0·5 etc., up to the final value $\alpha = 1{\cdot}0$ when the total depth $(h+\zeta)$ was taken into account. This procedure was time consuming but gave correct values for the parent model.

The initial runs of the Morecambe Bay model, however, using the above modification, gave completely unsatisfactory results. Unexpectedly high elevations, showing no signs of converging to the correct values, were found at various points of the model. So a series of tests was carried out to find the cause of these spurious values.

A smaller Morecambe Bay model was prepared and a series of runs carried out with various timesteps, alternative open boundaries, different open boundary input values, and a resmoothed depth distribution including and excluding areas of shallowest water. None of these changes gave satisfactory results.

The value of the friction parameter used throughout was 0·0025 as given by Proudman (1953) for open sea areas. Since Morecambe Bay contains large areas of very shallow water it seemed possible that a larger value might be appropriate. A further series of tests was thus implemented to investigate the effect of an increased friction parameter. These runs were carried out using the small Morecambe Bay model. This model, Morecambe Bay proper, contains exactly the same area as the hydraulic model being used at H.R.S., Wallingford. In the first run the friction parameter was increased by a factor of 10, i.e. $K_b = 0{\cdot}025$ and this removed the previous instability. The elevation values gave a smooth representation of the M_2 wave. This result encouraged further tests which indicated that, when considering very shallow waters, the friction coefficient should be increased by a factor of 3 to 4. The best results for Morecambe Bay proper were in fact obtained with $K_b = 0{\cdot}0075$. It has to be mentioned here that the parameter α may be given the value 1 throughout the calculation when K_b is increased in this way.

10·1 The parent model results

The first runs of the parent model were carried out, as described earlier, on the grid net shown in Figure 4. This matrix of grid points includes the first barrage crossings in Solway Firth and Morecambe Bay, excluding the most shallow parts of these estuaries.

The M_2 wave in question is shown in the enclosed Figure 19. The figure gives the distribution of the M_2 tide in the eastern Irish Sea at the time of high water at Liverpool.

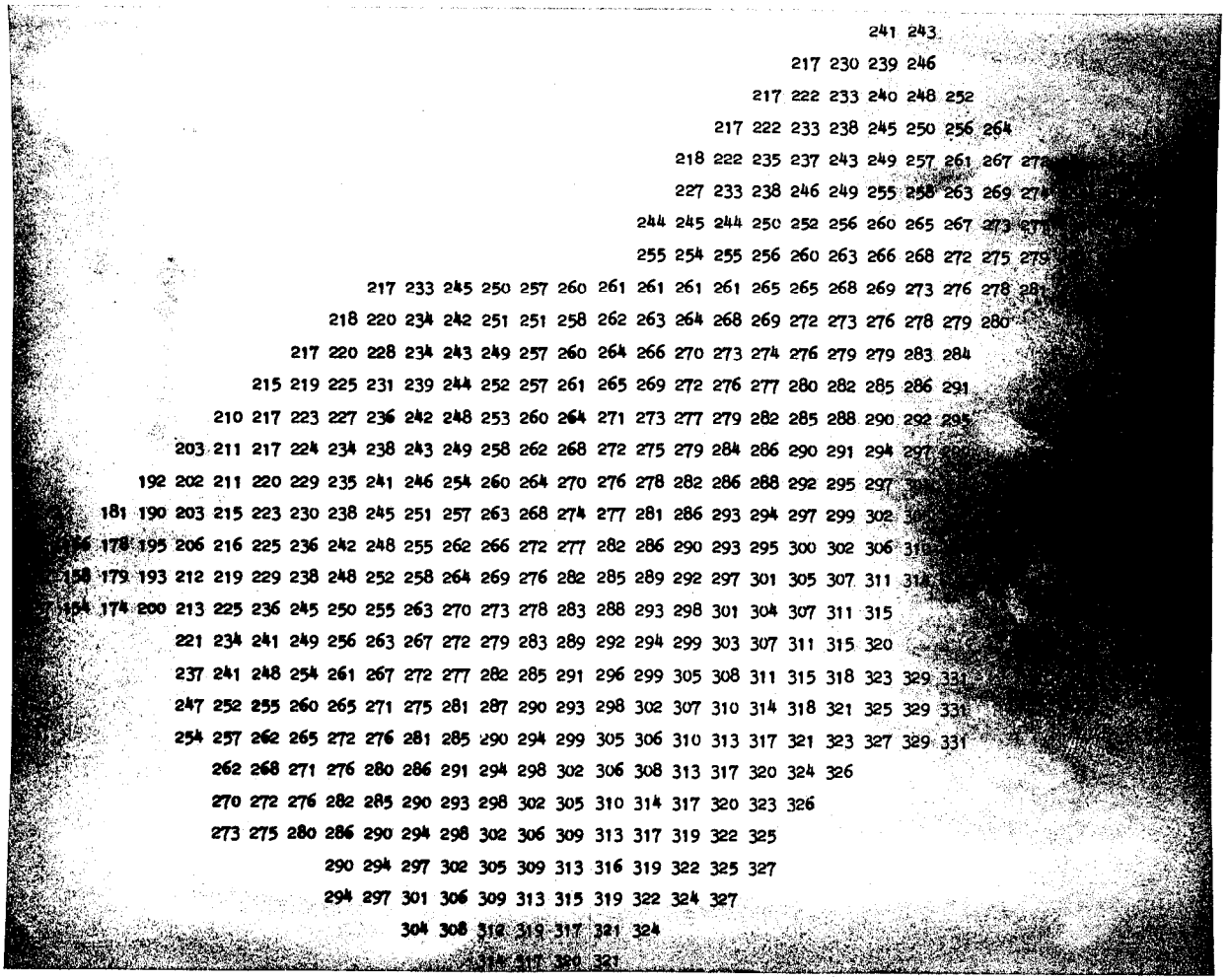

Figure 19. The elevations of M_2 tide in the eastern area of the Irish Sea at time of high water at Liverpool.

Comparison of the results obtained with those given in the co-tidal chart (Figure 2) shows that the H-N model reproduced the M_2 constituent with sufficient accuracy.

The enclosed table shows a comparison, for some of the main coastal stations, of the calculated amplitudes and those obtained by harmonic

analyses evaluated from the observed tidal data.

Table 1.

Tide gauge and the reference number of the elevation point in the model sea (Fig.2 and 4)		Amplitudes (cm)	
		Observed	Calculated
Birkenhead	(946)	319	321
Heysham	(738)	327	331
Walney Island	(643)	310	315
Workington	(276)	374	382
Sotherness	(217)	292	290
Abbey Head	(118)	270	264
Burrow Head	(84)	225	230
Ramsey	(234)	226	227
Douglas	(292)	230	233
Langness	(290)	230	233

A full comparison between the calculated elevations and the existing co-tidal chart can be made when, from all the theoretical data obtained from the H-N model, the harmonic constants (H) and (g) have been evaluated and a new co-tidal chart prepared. Such calculations are already being carried out using Doodson's filters, enabling the amplitudes and phases of the M_2 constituent and also the shallow water M_4, M_6 and M_8 constituents to be found.

Of course one has to bear in mind that any strict comparison of the tidal amplitudes (observed and calculated) cannot be fully achieved, for some of the tide gauges are situated inland and far away from the elevation point taken for comparison.

In order to demonstrate the current distribution of the M_2 tide the following two Figures (20 and 21) are given. The figures show the current pattern of the semi-diurnal tide 3 hours before and 3 hours after high water at Liverpool. This is to give a brief insight into the inflow and outflow of the sea water into the basin under consideration.

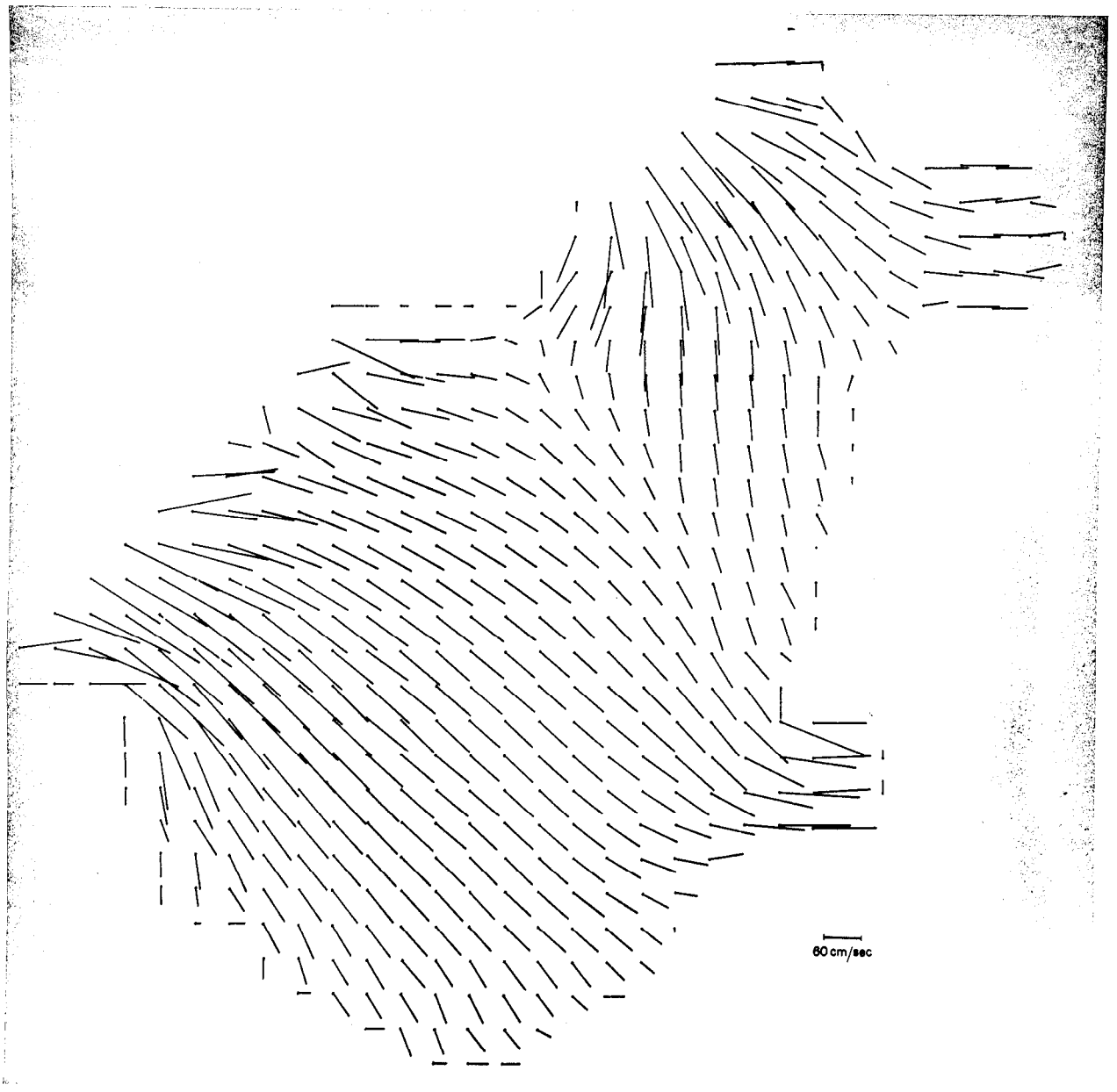

Figure 20. Resultant depth mean currents in the eastern Irish Sea area 3 hours before high water at Liverpool.

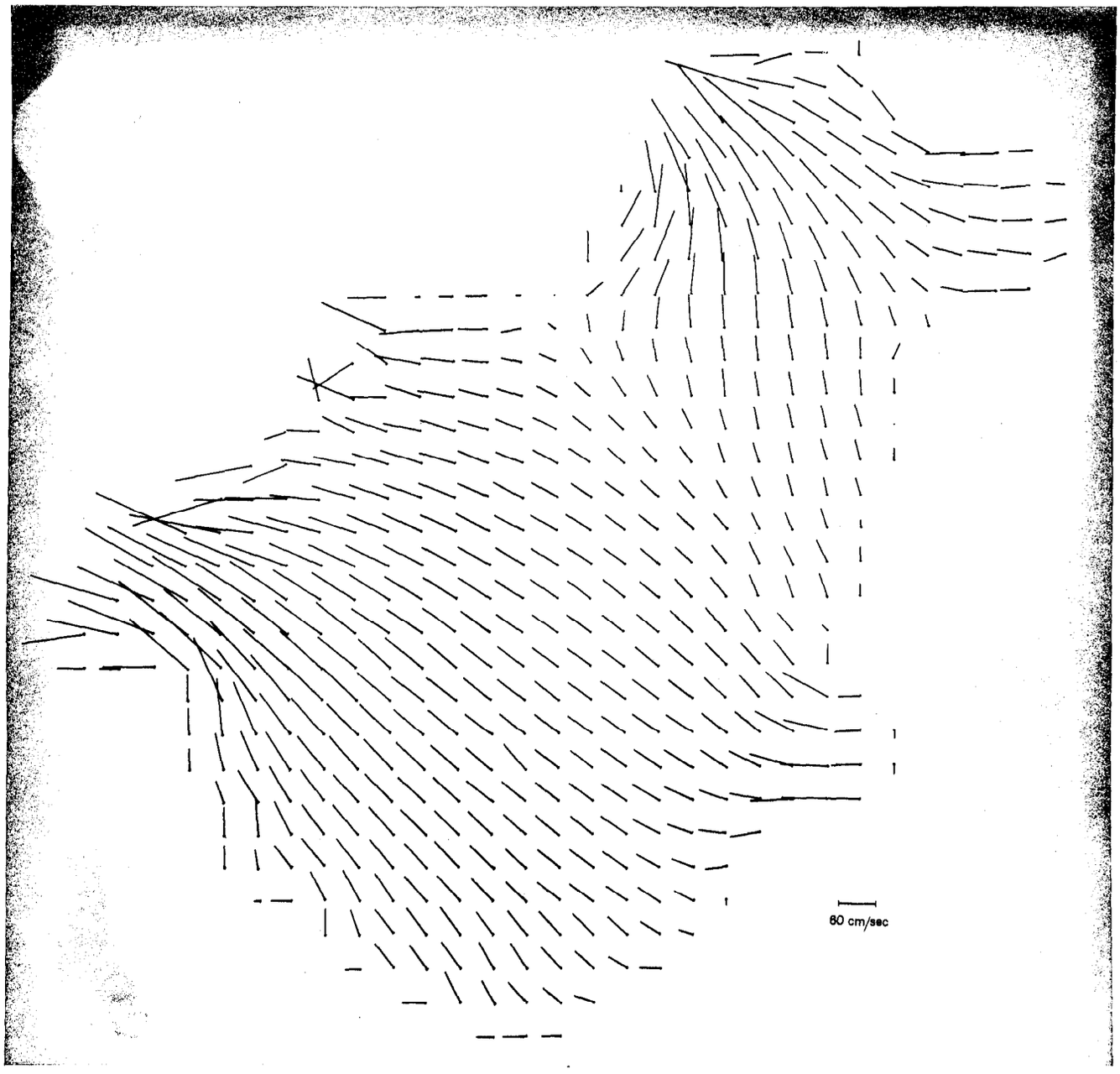

Figure 21. Resultant depth mean currents in the eastern Irish Sea area 3 hours after high water at Liverpool.

Although the figures show the depth mean current only, the representation of the tidal current gives a fair picture of the water movements in the eastern area of the Irish Sea.

As mentioned earlier the tidal currents enter the eastern Irish Sea, as seen from the enclosed Figure 20, through two entraces, north and south of the Isle of Man. There the currents are strongest reaching up to 180 cm/sec. Going further into the basin one can see that the velocity of the resultant depth mean current weakens and in average reaches about 60 cm/sec. A distinct increase in the current velocity can be seen again in the inner parts of the main estuaries; Solway Firth and Morecambe Bay.

Analysing the currents of the M_2 tide it can easily be seen that two separate areas in the current pattern occur. The water masses entering the eastern Irish Sea through the southern and northern passage build in some way their own reservoirs between which a small water exchange occurs; neglecting here of course any wind effect. An apparent separation of the two water masses follows roughly on the line between Barrow and Ramsey.

More detailed information concerning the current pattern can be given when a current picture has been laid out showing the current distribution in different stages of the tide, i.e. in a full cycle of the tidal wave.

Another diagram follows (Figure 22) to show briefly the M_2 wave for some elevation points, of the H-N model, which may be referred to the tide gauge stations chosen: Workington, Douglas, Heysham and Birkenhead.

Here the full tidal range is shown. Many diagrams, with the tidal curves, were drawn for different places showing that the shallow water effect produces, for some tidal stations, a higher amplitude for high water and lower for low water. Thus, instead of tidal amplitudes one should speak about the half range of the tide. This difference in interpretation could account for the small discrepancies shown in Table 1.

Another interesting feature has been observed, on the diagrams prepared, that a distinct influence of the shallow water effect (non-linear terms in the equations of motion) was shown in a faster rise and slower fall of the vertical displacement of the water; see elevation points, in particular 738 -Heysham and 946 -Birkenhead.

The following diagram (Figure 23) displays the parent model extended (no barrier case) by including very shallow water areas in Solway Firth and Morecambe Bay. The depth distribution for this matrix is given in Figure 24, and includes the innermost parts of the mentioned estuaries with an 'artificial' bathymetry in some places (the water volume, however, was maintained as far as possible). This was necessary in order to show any differences in elevations obtained running the parent model with a barrier and without a barrier.

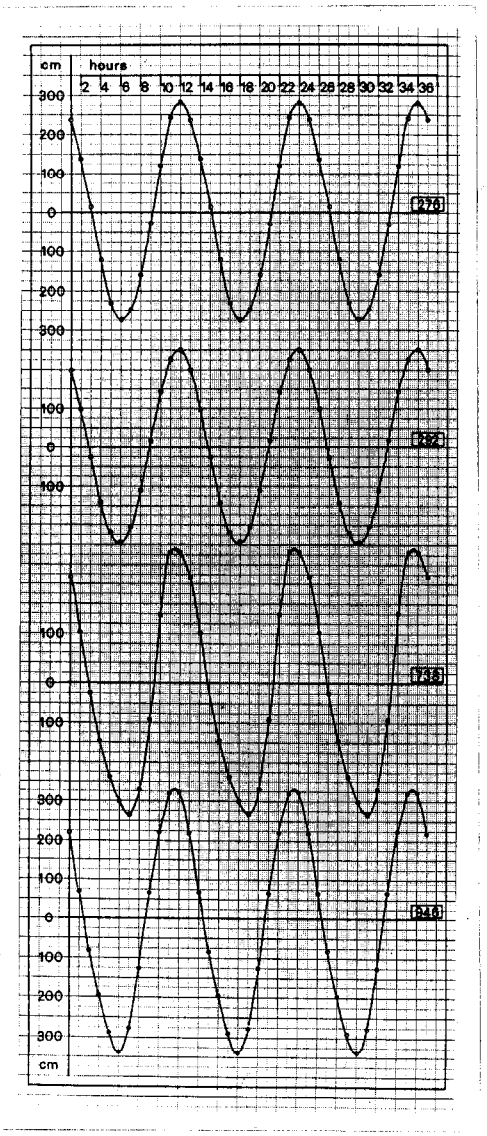

Figure 22. Tidal curve of the M_2 constituent at four elevation points:
276 -Workington,
292 -Douglas,
738 -Heysham and
946 -Birkenhead.

The main interest in running the extended parent model was focused on the elevations lying approximately along the open boundary (see elevation points: 668,669,701, 702, 703, 735, 769, 803, 837 and 871) chosen for hydraulic model investigations.

A comparison between the elevation values obtained from both models (barrier and no barrier case), taking into account the half range of the M_2 tide, has been carried out, showing a 4·5% increase in the elevations of the non-barrier case over those obtained previously, i.e. when the barriers were introduced.

It has to be emphasised that the given conclusion cannot be fully accepted for the extended parent model did not give satisfactory results (as might be expected anyway in giving artificial depth values in places where drying banks occur already during mean tide) as far as the rest of the Irish Sea area was concerned. Therefore another run was carried out with barrage crossings placed approximately (see Figure 23) at the main entrances to Solway Firth and Morecambe Bay avoiding completely the shallow estuarial waters. Here another decrease in water elevations resulted, apparently showing that the exclusion of the shallow estuarial waters gives slightly smaller amplitudes along the coast.

The last model of the whole series of parent models gave the most reliable results; proving once more the full usefulness of the H-N method to open sea areas.

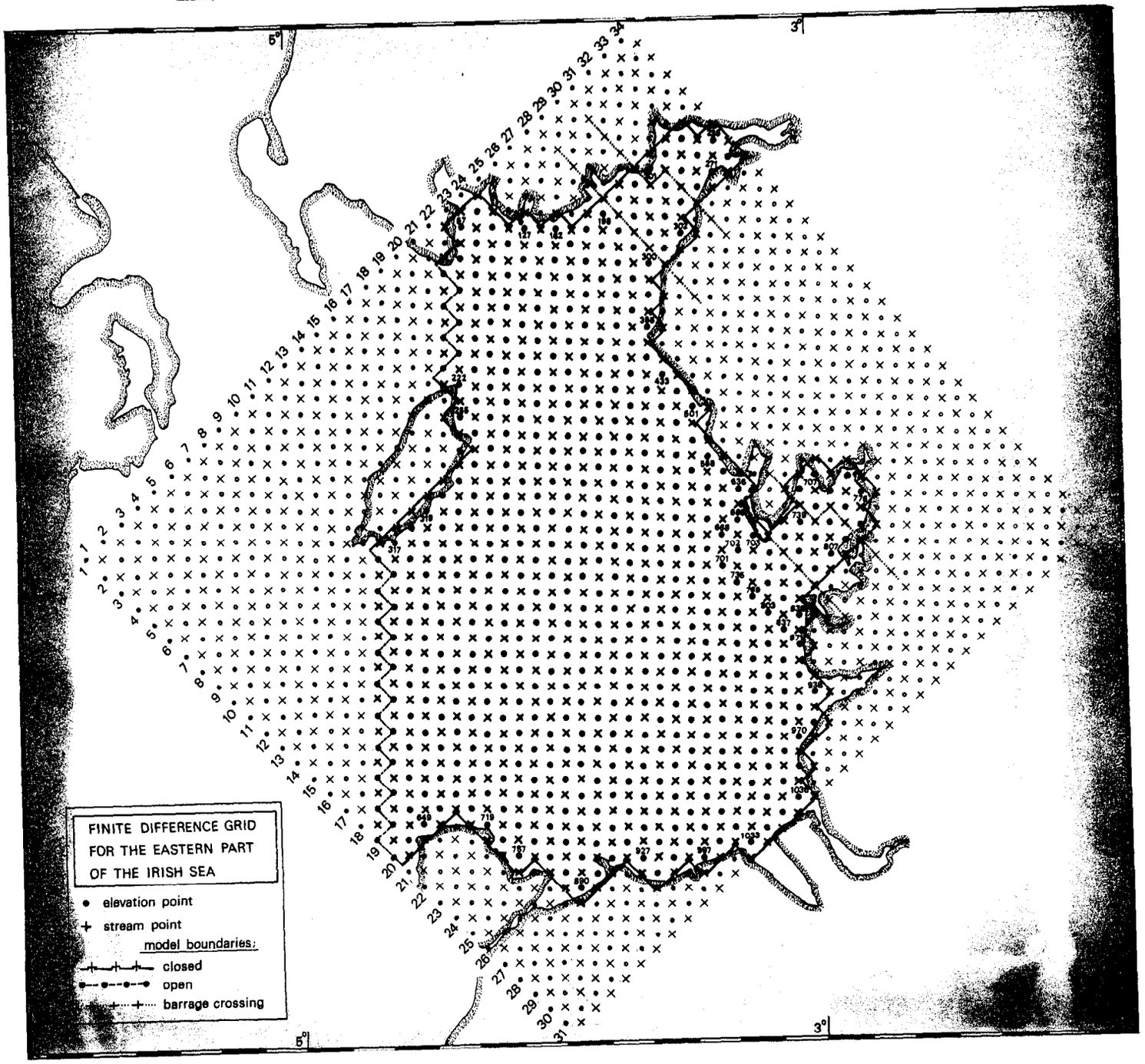

Figure 23. Grid net of the parent model extended, showing the position of two barrage crossings in Morecambe Bay and Solway Firth. Numbers at various places indicate the seeking elevation values at the open boundary of the hydraulic model and elevation values at some of the coastal stations.

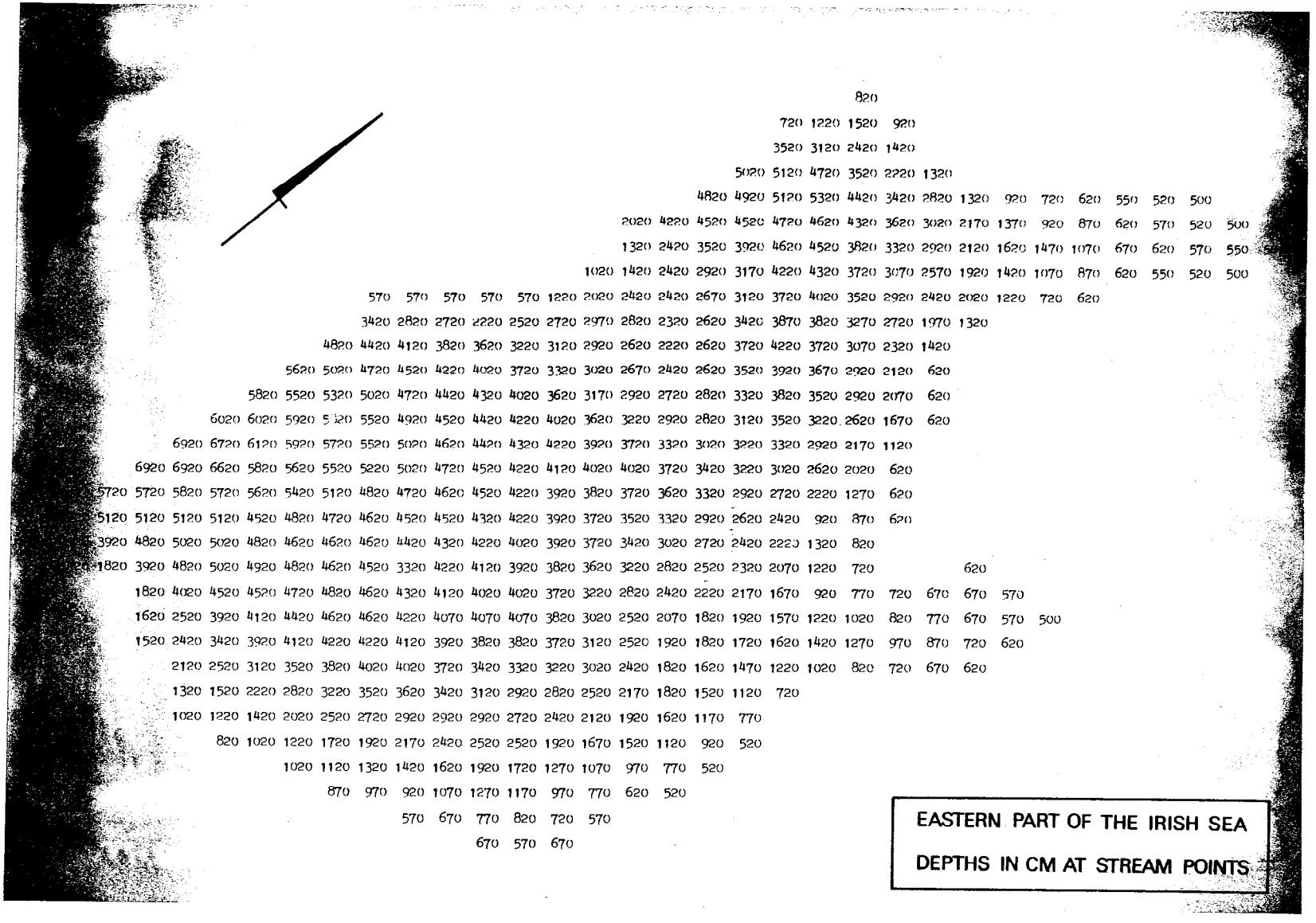

Figure 24. Depth distribution in the eastern part of the Irish Sea for the parent model extended.

A comparison of the two diagrams (Figure 16 and 24) shows that the depth distribution at the latter was resmoothed in some way. The depth values along the land boundaries were slightly increased and the innermost parts of the estuaries were given (in some places) fictitious depth values. This provided the possibility of running the parent model without a barrier, and the increased depths, along the coasts enabled the extended model to be run without introducing the α parameter, thus saving a lot of computer time. But as mentioned already the results obtained for the parent model extended, cannot be fully accepted and really little can be said as far as the differences in elevation at the open boundary of the hydraulic model are concerned.

More detailed and reliable information of the barrage influence on the open boundary of the hydraulic model was found by running the Morecambe Bay model. General information about the results is given in the following paragraph.

10.2 The Morecambe Bay model results

A thorough discussion of the Morecambe Bay results will be given in a separate report, however a general layout and short insight into some of the results obtained is given here.

The runs for the main Morecambe Bay model were carried out on the difference grid shown in figure 25.

The open boundary input was fed into the model at the outer elevation points.

Due to the introduction of the innermost parts of the estuary, areas beyond the barrage crossing, it was desirable to use a friction parameter as high as $k_b = 0{\cdot}01$. The application of the high friction parameter enabled us to neglect the α parameter and the results obtained were, as will be seen, quite satisfactory.

The depth distribution used in our calculations is given in figure 26.

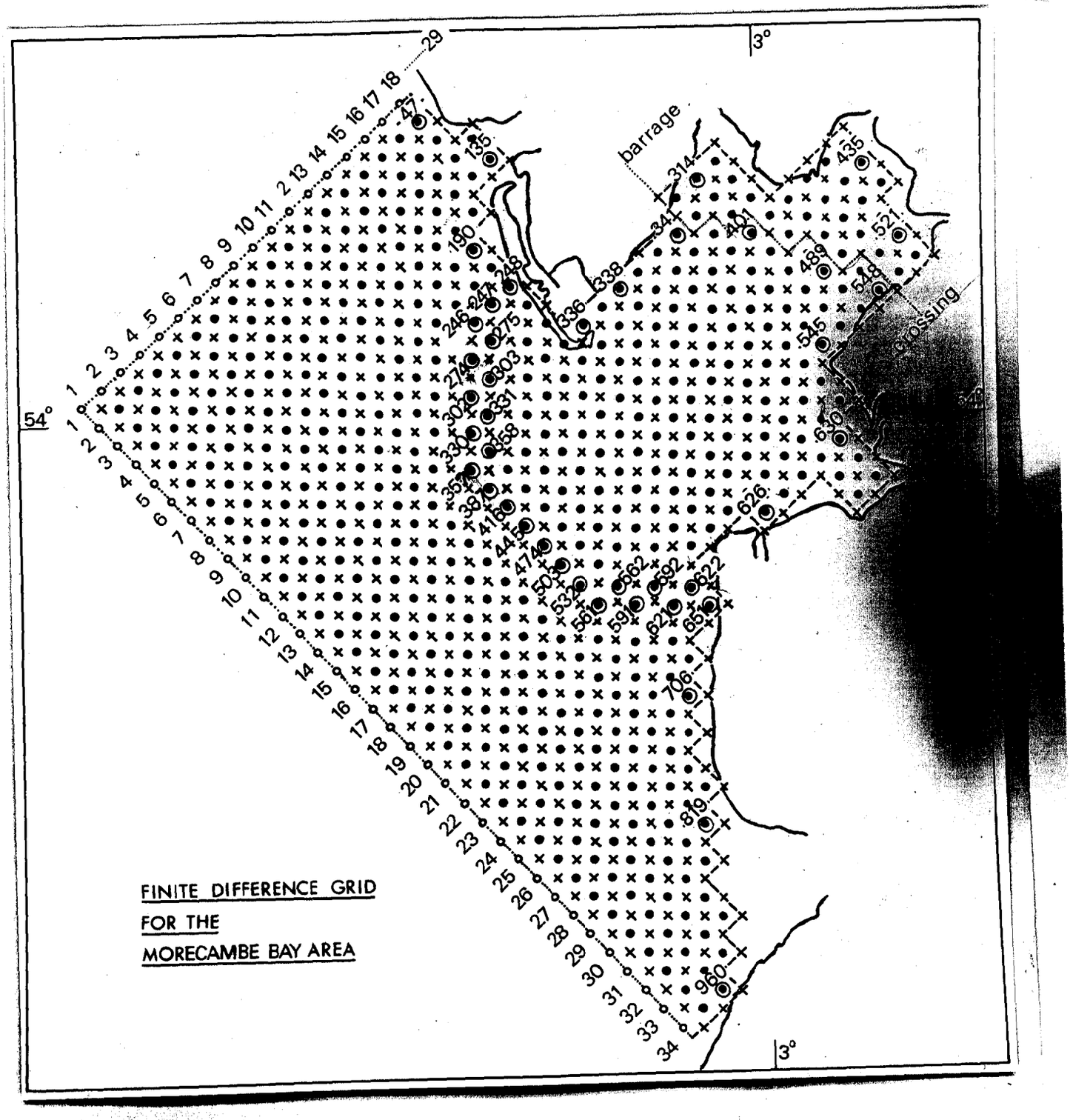

Figure 25. Finite-difference grid for the Morecambe Bay model.

Numbers at circled points indicate the approximate open boundary alignment of the hydraulic model investigations and the seeking elevation values for some of the coastal stations.

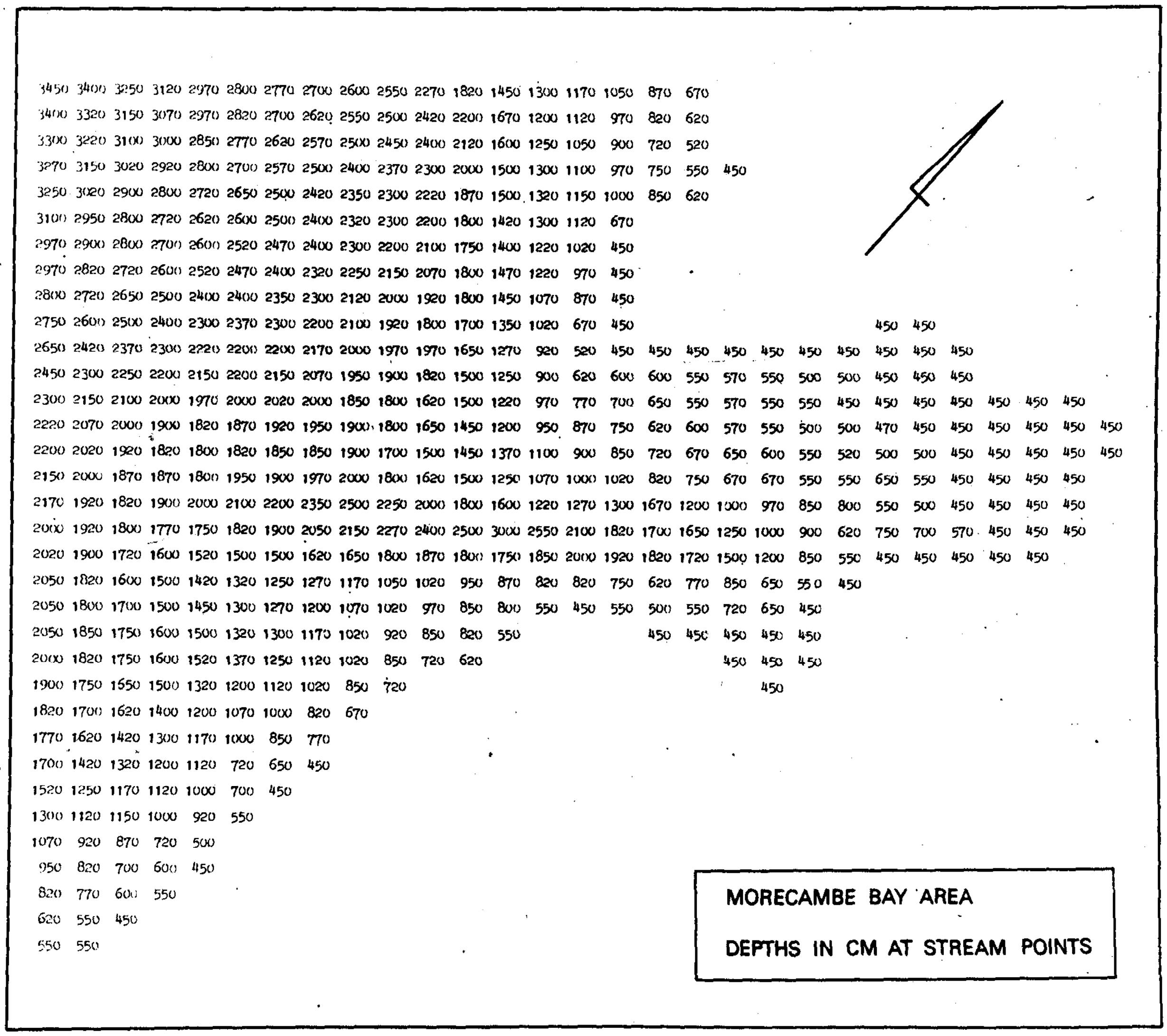

Figure 26. Depth distribution in the Morecambe Bay model.

In all three runs were perfprmed for the Morecambe Bay model under discussion. Additional runs were carried out for the model of Morecambe Bay proper but they are not being discussed here.

The first run of the large Morecambe Bay model was carried out for the total water basin covered by the mesh in figure 25. The second run covered the same sea area but without Coriolis parameter. The third one was carried out with a barrage crossing - excluding the shallowest parts of the Morecambe Bay estuary.

Figure 27 shows the distribution of the calculated M_2 wave during high water at Heysham, so that figure 27A gives the elevations without and figure 27B with a barrier crossing.

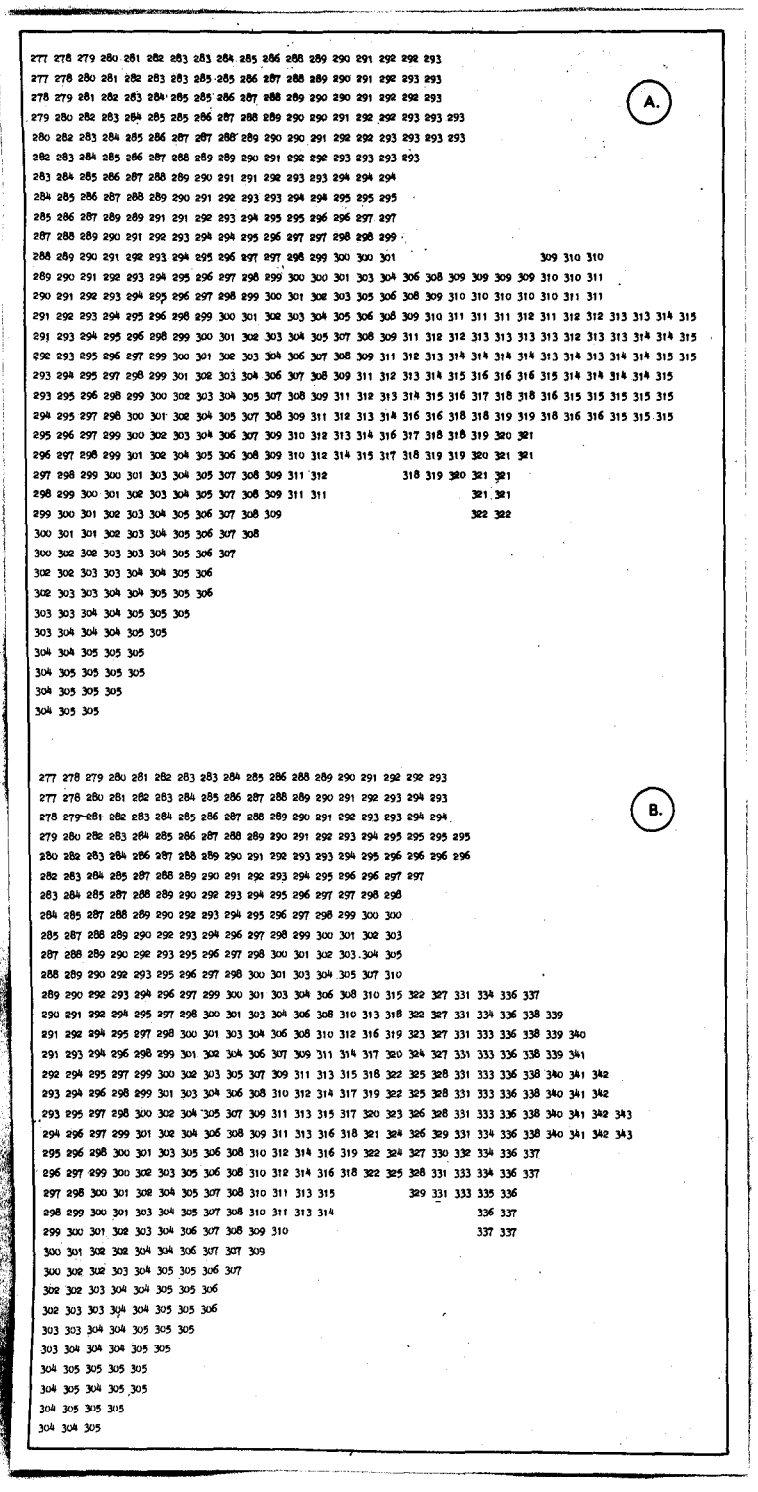

A.

277 278 279 280 281 282 283 283 284 285 286 288 289 290 291 292 292 293
277 278 280 281 282 283 283 285 285 286 287 288 289 290 291 292 293 293
278 279 281 282 283 284 285 285 286 287 288 289 290 290 291 292 292 293
279 280 282 283 284 285 285 286 287 288 289 290 290 291 292 292 293 293 293
280 282 283 284 285 286 287 287 288 289 290 290 291 292 292 293 293 293 293
282 283 284 285 286 287 288 289 289 290 291 292 292 293 293 293 293
283 284 285 286 287 288 289 290 291 291 292 293 293 294 294 294
284 285 286 287 288 289 290 291 292 293 293 294 294 295 295 295
285 286 287 289 289 291 291 292 293 294 295 295 296 296 297 297
287 288 289 290 291 292 293 294 294 295 296 297 297 298 298 299
288 289 290 291 292 293 294 295 296 297 297 298 299 300 300 301 309 310 310
289 290 291 292 293 294 295 296 297 298 299 300 300 301 303 304 306 308 309 309 309 309 310 310 311
290 291 292 293 294 295 296 297 298 299 300 301 302 303 305 306 308 309 310 310 310 310 310 311 311
291 292 293 294 295 296 298 299 300 301 302 303 304 305 306 308 309 310 311 311 311 312 311 312 312 313 313 314 315
291 293 294 295 296 298 299 300 301 302 303 304 305 307 308 309 311 312 312 313 313 313 313 312 313 313 314 314 315
292 293 295 296 297 299 300 301 302 303 304 306 307 308 309 311 312 313 314 314 314 314 313 314 313 314 314 315 315
293 294 295 297 298 299 301 302 303 304 306 307 308 309 311 312 313 314 315 316 316 316 315 314 314 314 314 315
293 295 296 298 299 300 302 303 304 305 307 308 309 311 312 313 314 315 316 317 318 318 316 315 315 315 315 315
294 295 297 298 300 301 302 304 305 307 308 309 311 312 313 314 316 316 318 318 319 319 318 316 316 315 315 315
295 296 297 299 300 302 303 304 306 307 309 310 312 313 314 316 317 318 318 319 320 321
296 297 298 299 301 302 304 305 306 308 309 310 312 314 315 317 318 319 319 320 321 321
297 298 299 300 301 303 304 305 307 308 309 311 312 318 319 320 321 321
298 299 300 301 302 303 304 305 307 308 309 311 311 321 321
299 300 301 302 303 304 305 306 307 308 309 322 322
300 301 301 302 303 304 305 306 307 308
300 302 302 303 303 304 305 306 307
302 302 303 303 304 304 305 306
302 303 303 304 304 305 305 306
303 303 304 304 305 305 305
303 304 304 304 305 305
304 304 305 305 305
304 305 305 305 305
304 305 305 305
304 305 305

B.

277 278 279 280 281 282 283 283 284 285 286 288 289 290 291 292 292 293
277 278 280 281 282 283 284 285 286 287 288 289 290 291 292 293 294 293
278 279 281 282 283 284 285 286 287 288 289 290 291 292 293 293 294 294
279 280 282 283 284 285 286 287 288 289 290 291 292 293 294 295 295 295 295
280 282 283 284 286 287 288 289 290 291 292 293 293 294 295 296 296 296 296
282 283 284 285 287 288 289 290 291 292 293 294 295 296 296 297 297
283 284 285 287 288 289 290 292 293 294 295 296 297 297 298 298
284 285 287 288 289 290 292 293 294 295 296 297 298 299 300 300
285 287 288 289 290 292 293 294 296 297 298 299 300 301 302 303
287 288 289 290 292 293 295 296 297 298 300 301 302 303 304 305
288 289 290 292 293 295 296 297 298 300 301 303 304 305 307 310
289 290 292 293 294 296 297 299 300 301 303 304 306 308 310 315 322 327 331 334 336 337
290 291 292 294 295 297 298 300 301 303 304 306 308 310 313 318 322 327 331 334 336 338 339
291 292 294 295 297 298 300 301 303 304 306 308 310 312 316 319 323 327 331 333 336 338 339 340
291 293 294 296 298 299 301 302 304 306 307 309 311 314 317 320 324 327 331 333 336 338 339 341
292 294 295 297 299 300 302 303 305 307 309 311 313 315 318 322 325 328 331 333 336 338 340 341 342
293 294 296 298 299 301 303 304 306 308 310 312 314 317 319 322 325 328 331 333 336 338 340 341 342
293 295 297 298 300 302 304 305 307 309 311 313 315 317 320 323 326 328 331 333 336 338 340 341 342 343
294 296 297 299 301 302 304 306 308 309 311 313 316 318 321 324 326 329 331 334 336 338 340 341 342 343
295 296 298 300 301 303 305 306 308 310 312 314 316 319 322 324 327 330 332 334 336 337
296 297 299 300 302 303 305 306 308 310 312 314 316 318 322 325 328 331 333 334 336 337
297 298 300 301 302 304 305 307 308 310 311 313 315 329 331 333 335 336
298 299 300 301 303 304 305 307 308 310 311 313 314 336 337
299 300 301 302 303 304 306 307 308 309 310 337 337
300 301 302 302 304 304 306 307 307 309
300 302 302 303 304 305 305 306 307
302 302 303 304 304 305 305 306
302 303 303 304 304 305 305 306
303 303 304 304 305 305 305
303 304 304 304 305 305
304 305 305 305 305
304 305 304 305 305
304 305 305 305
304 304 305

Figure 27. Distribution of the M_2 wave in the Morecambe Bay model.
(A - without a barrier, B - with a barrier.)
Values taken to the nearest centimetre.

It is apparent that the introduction of a barrier crossing gave a slight increase in elevations along the open boundary of the hydraulic model. Greater increases of elevation are noticed however along the barrier itself. Encouraging is the fact that almost no differences are revealed along the open coast, showing that a barrier introduced in Morecambe Bay will not seriously influence the water elevations in these areas, i.e. north of Walney Island and south of Fleetwood.

The following figure (Figure 28) gives the water elevations for a run in which the Coriolis force has been neglected.

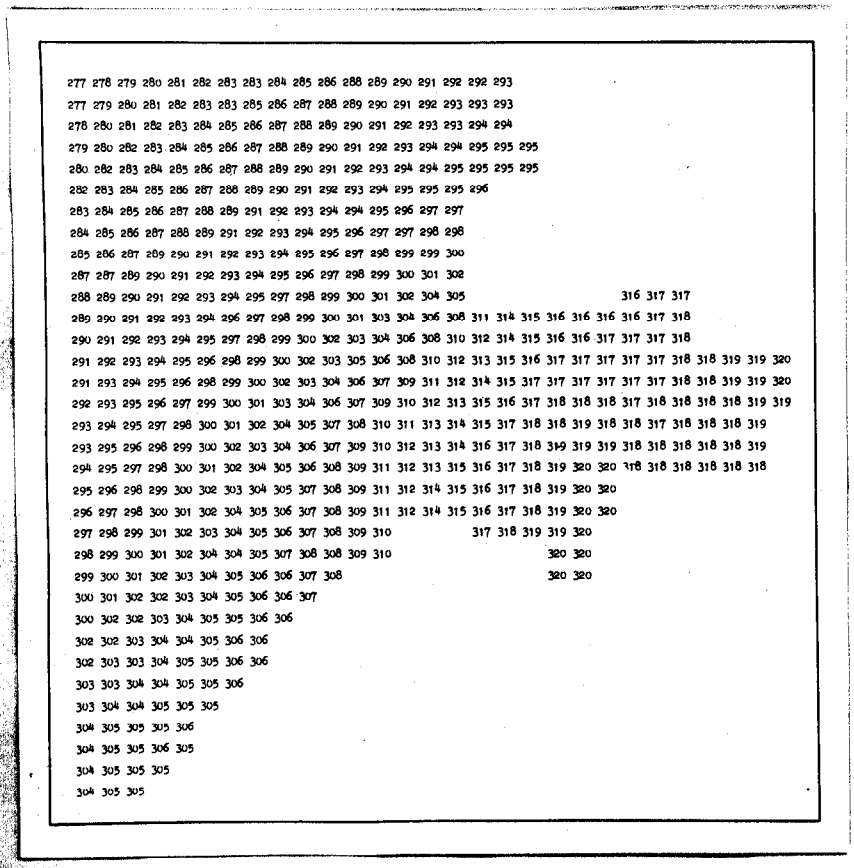

Figure 28. Distribution of the M_2 wave in the Morecambe Bay model when the Coriolis effect is neglected.

Comparing this diagram with the one of 27A it can be noticed that a small gradient of elevation occurs when a Coriolis effect is introduced. But it can be said that the Coriolis force does not make a great influence on the water elevations as such and could be neglected as far as the engineering aspect is concerned. Perhaps a greater influence of the Coriolis effect will be found when considering the current pattern, but this will be discussed later on.

A rough estimate based on the comparison of the elevation output values, for the Morecambe Bay proper, indicates that the best reproduction of the M_2 wave could be achieved when the k_b coefficient is between 0·0075 and 0·01, say, k_b = 0·0090. The latter value, although high in comparison with the Proudman's (1953) value 0·0025, seems quite reasonable for shallow water areas as those in Morecambe Bay estuary.

Figure 29 shows the increase in elevation along the open boundary of the hydraulic model upon introduction of the barrier, Coriolis effect being included. From figure 27a and 29 it can be seen that the effect of the barrier is to increase elevations along the open boundary of the hydraulic model by 2%. A comparison of figures 27A and 27B shows that the increase in elevation at points adjacent to the barrier location is of order 9%.

The effect of omitting Coriolis force on elevations along the hydraulic model open boundary is shown in figure 30 for the no barrier case.

The barrier introduction gave only a very slight increase (negligible from the engineering point of view) in elevation along the open boundary of the hydraulic model. This shows that the open boundary of the H.R.S. model was well chosen. As the figure indicates a smaller increase of elevations might be expressed when Coriolis force is neglected which of course is the case in the H.R.S. model.

But see letter of 19th June, 1970, reference 0501/JRR/PMC and new figs. 29 and 30.

11. General concluding remarks

The calculations carried out so far proved quite satisfactory in spite of the shallow water problems involved. In particular the reproduction of the tidal elevations is encouraging. Some doubts however remain concerning the phases of the M_2 tide.

An introductory analysis shows that the phase differences are a bit larger than they should be in comparison with the values obtained from I.C.O.T. harmonic analyses. This discrepancy is due perhaps mainly to the application of the high friction parameter used in our calculations. One should be aware also that the elevation values obtained numerically include, due to the non-linearity of the model, the higher harmonics i.e. M_4, M_6 and M_8.

A full discussion of the results obtained can be given when these constituents have been evaluated.

It seems probable that a variable friction parameter, with a low value in the open sea increasing in the shallower parts of the model, could further improve the results.

Improvements could also be achieved by introducing into the programming technique the problem of drying banks so that zero values of the total depth would be permitted.

The computer used also posed some difficulties. A 24 hour simulation of the M_2 wave for the Morecambe Bay model took about 60 minutes of computer time. This was one of the reasons for the Dee River model (with its very fine mesh and short timesteps) being discarded for the moment.

Although the results, from numerical model investigations, are encouraging no complacancy should so far be shown, for still a lot has to be done in achieving fully acceptable predictions of water movements, of astronomical and meteorological origin, in estuarial waters, where a complex interaction among different forces and their responses is observed.

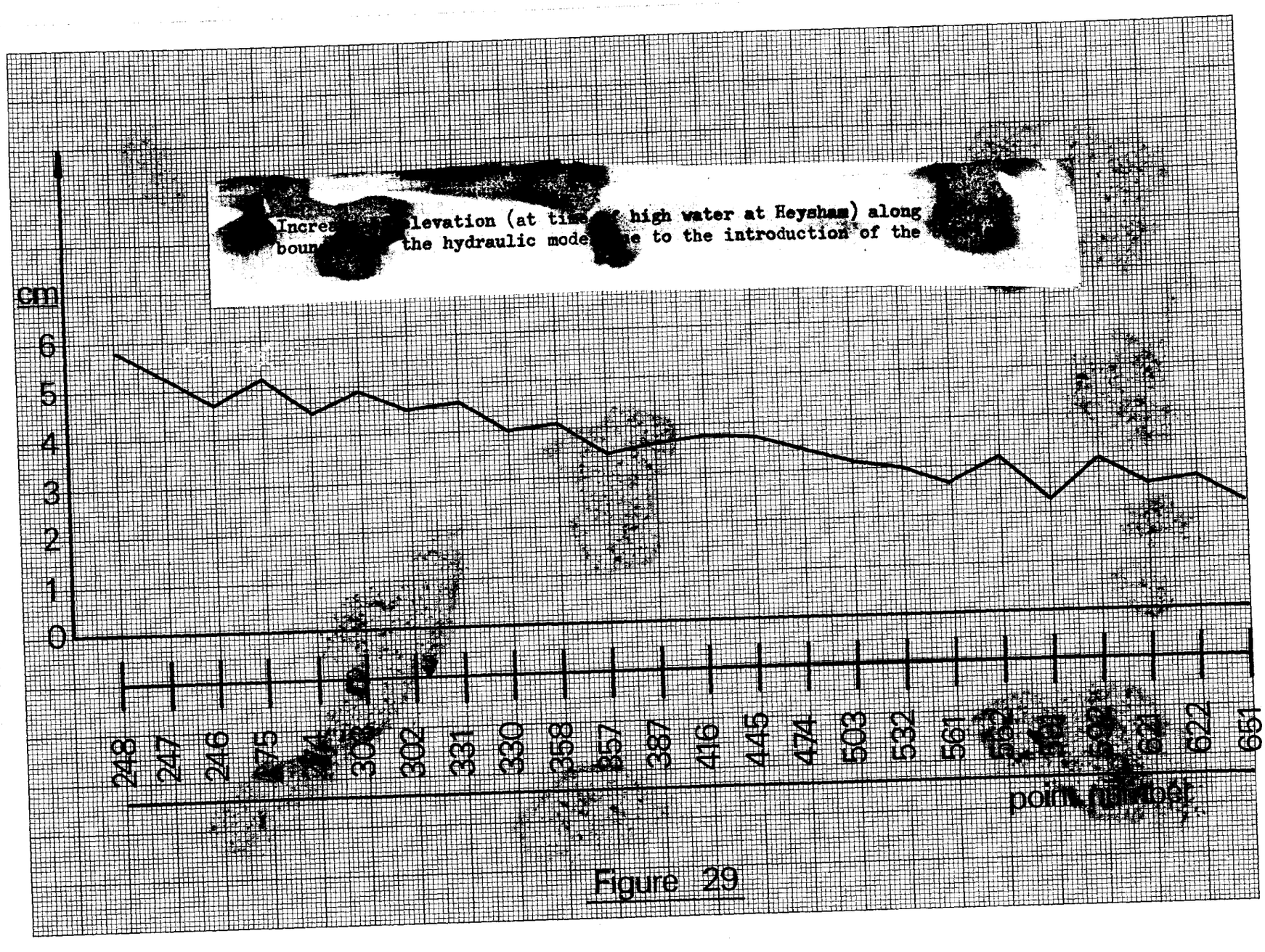
Increase in elevation (at time of high water at Heysham) along the boundary of the hydraulic model due to the introduction of the
cm
6
5
4
3
2
1
0
248
247
246
245
331
330
416
445
474
503
532
561
622
651
point number

Figure 29

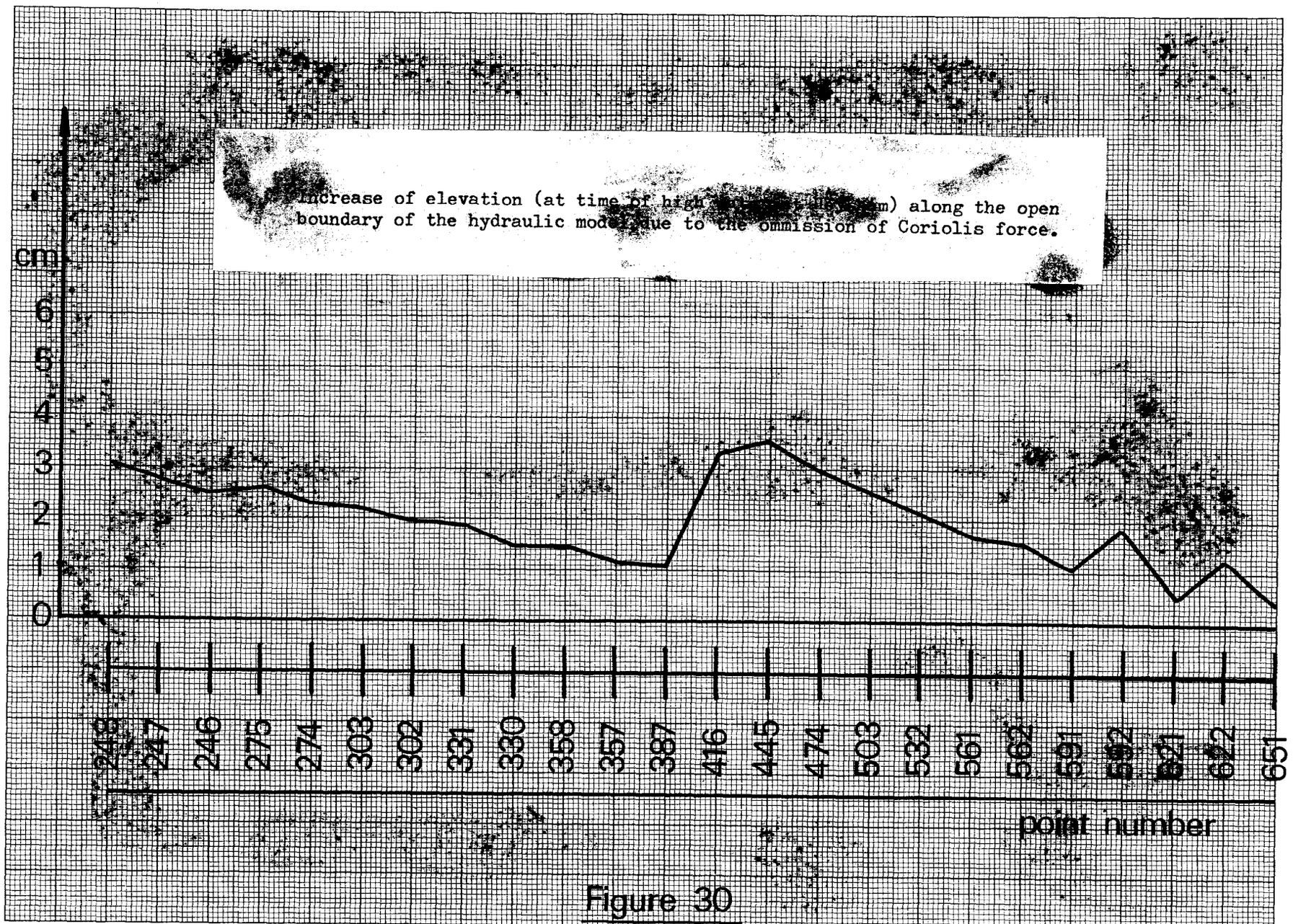
Increase of elevation (at time of high
m) along the open
boundary of the hydraulic mode
ue to the ommission of Coriolis force.
cm
6
5
4
3
2
1
0
248
247
246
275
274
303
302
331
330
358
357
387
416
445
474
503
532
561
590
591
592
621
622
651
point number

Figure 30

Acknowledgement

My sincere thanks are due to Dr. J.R. Rossiter, Director of the Institute of Coastal Oceanography and Tides, supervisor of the research, for the confidence he has shown in giving me the barrage problem and for his ceaseless, patient advice and interest throughout the work.

I am deeply indebted to Miss J.E. Banks, Mr N.S. Heaps and Mr R.A. Flather for their assistance, help and advice in carrying out the calculations.

Great appreciation is given to all members of the I.C.O.T. staff who, by their help and friendship, made the author's stay on 'Bidston Hill' most fruitful and pleasant. Thanks are also due to the Natural Environment Research Council for the Research Grant given to carry out the research.

Last but not least my grateful acknowledgement is made to my wife Mira who gave up, for two years, her medical profession to look after our newly established home and shared with me all the inevitable ups and downs.

References

Banks, J. E., (1967) A numerical model to study tides and surges in a river-shallow sea combination. M.Sc. Thesis, University of Liverpool.

Bonnefille, R., (1969), Contribution théorique et expérimentale à l'étude du regime des marées. Bull. de la Direction des Études et Recherches, Série A.1.

Buckingham, R. A. (1957), Numerical Methods. J. Pitman Ltd., London.

Collatz, L., (1960), Metody numeryczne rozwiazywania równań różniczkowch. P. W. N. Warszawa.

Courant, R., Friedrichs, K. O. and Lewy, H., (1928) Über die Partiellen Differencen-Gleichungen der Mathematischen Physik. Math. Ann. 100.

Defant, A., (1961), Physical Oceanography, Vol. I, Pergamon Press, Oxford.

Doodson, A. T., (1928), The analysis of tidal observations. Phil. Trans. A.227.

Doodson, A. T. and Corkan, R. H. (1932), The principal constituent of the tides in the English and Irish channels. Phil.Trans.R.Soc. A.231.

Doodson, A. T., Rossiter, J. R. and Corkan, R. H., (1954). Tidal charts based on coastal data : Irish Sea. Proc. Roy. Soc. of Edinburgh, Sec. A.LXIV.

Dooley, H. D. and Steele, J. H., (1969), Wind driven currents near a coast, Dt. Hydrogr. Z.22.

Dronkers, J. J., (1964), Tidal computations in river and coastal waters. North Holland Publ. Co., Amsterdam.

Fischer, G., (1959), Ein numerisches Verfarhen zur Errechnung von Windstau und Gezeiten in Randmeeren, Tellus, 11.

Greenberg, D. A., (1969), Modification of the M_2 tide due to barriers in the Bay of Fundy, J.Fish.Res. Bd. Canada, 26.

Hansen, W., (1956), Theorie zur Errechnung des Wasserstandes und der Strömungen in Randmeeren nebst Anwendungen. Tellus, 8.

Hansen, W., (1966), The influence of coastal engineering structures on tides, currents and wind effects. Dock and Harbour Authority. XLVII.

Harris, D. L. and Jelesnianski, C. P. (1964), Some problems involved in the numerical solution of tidal hydraulics equations. Monthly Weather Rev. 92.

Heaps, N. S. (1968), Estimated effects of barrage on tides in the Bristol Channel, Proc. Inst. Civ. Engrs., 40.

Heaps, N. S. (1969), A two-dimensional numerical sea model. Phil. Trans. A.1160.

Hughes, P., (1969), Submarine cable measurements of tidal currents in the Irish Sea. Limn. and Oceanography, 14.

Lauwerier, H. A., (1961), Some recent work of the Amsterdam Mathematical Centre on the hydrodynamics of the North Sea. Proc. Symp. on Math. Hydrod. Methods of Phys. Oceanography, Sept. 1961.

Lennon, G. W. (1963), A frequency investigation of abnormally high tidal levels at certain west coast ports. Proc. Inst, of Civ. Engrs. 25.

Phillips, A., (1969), Sea-bed water movements in Morecambe Bay. Dock and Harbour Auth. XLIX.

Proudman, J., (1953), Dynamical Oceanography, Methuen, London.

Raming, H. G., (1968), Ermittlung von Bewegungsvorgängen im Meere und Flussmündungen zur Untersuchung des Transportes von Verunreinigungen. Helgolander wiss. Meeresunters. 17.

Richtmyer, R. D.,(1957), Difference methods for initial-value problems. New York and London : Interscience Publishers.

Rossiter, J. R., (1961), Some numerical tidal problems. Proc.Symp. on Math. Hydrod. Methods of Phys. Oceanography, Sept. 1961.

Rossiter, J. R. and Lennon, G. W. (1968), An intensive analysis of shallow water tides, Geophys. J. R. Astr. Soc., 16.

Sager, G., (1964), Das Regime der Gezeiten und der Gezeitenströme in der Nordsee, dem Kanal und der Irishen See. Beiträge zur Meereskunde, Heft 11.

Sgibneva, L. A., (1966), Tide calculation in a sea of real shape. Oceanology 6.

Sverdrup, H. U., (1946), The Oceans, New York, Prentice-Hall, Inc.

Ueno, T., (1964), Non-linear numerical studies on tides and surges in the central part of Seto Island Sea. Ocean.Mag. Japan Met. Agency 16.

Welander, P., (1961), Numerical prediction of storm surges. Advances in Geophysics. 8.